



저작자표시-비영리-변경금지 2.0 대한민국

이용자는 아래의 조건을 따르는 경우에 한하여 자유롭게

- 이 저작물을 복제, 배포, 전송, 전시, 공연 및 방송할 수 있습니다.

다음과 같은 조건을 따라야 합니다:



저작자표시. 귀하는 원저작자를 표시하여야 합니다.



비영리. 귀하는 이 저작물을 영리 목적으로 이용할 수 없습니다.



변경금지. 귀하는 이 저작물을 개작, 변형 또는 가공할 수 없습니다.

- 귀하는, 이 저작물의 재이용이나 배포의 경우, 이 저작물에 적용된 이용허락조건을 명확하게 나타내어야 합니다.
- 저작권자로부터 별도의 허가를 받으면 이러한 조건들은 적용되지 않습니다.

저작권법에 따른 이용자의 권리는 위의 내용에 의하여 영향을 받지 않습니다.

이것은 [이용허락규약\(Legal Code\)](#)을 이해하기 쉽게 요약한 것입니다.

[Disclaimer](#)

DOCTOR OF PHILOSOPHY

**ARTIFICIAL INTELLIGENCE TECHNIQUES
FOR ROLLING ELEMENT BEARINGS FAULT DIAGNOSIS**



**The Graduate School
of the University of Ulsan**

**Department of Electrical, Electronic and
Computer Engineering**

Yangde Gao

**Artificial Intelligence Techniques
For Rolling Element Bearings Fault Diagnosis**

Dissertation

for the Degree of

Doctor of Philosophy

(Electrical, Electronic and Computer Engineering)

University of Ulsan

Yangde Gao

July 2024

Artificial Intelligence Techniques For Rolling Element Bearings Fault Diagnosis

Supervisor: Professor Jong–Myon Kim

A Dissertation

Submitted to
the Graduate School of the University of Ulsan
In partial Fulfillment of the Requirements
for the Degree of

Doctor of Philosophy

by

Yangde Gao

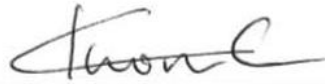
Department of Electrical, Electronic
and Computer Engineering

University of Ulsan,
Ulsan, Republic of Korea

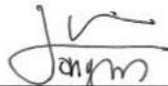
July 2024

Artificial Intelligence Techniques For Rolling Element Bearings Fault Diagnosis

This certifies that the dissertation
of Yangde Gao is approved.



Professor Kwon, YoungKeun, Committee Chair



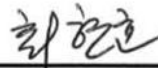
Professor Kim, Jong-Myon, Advisor



Professor Jo, Dongsik, Committee Member



Dr. Im, Kichang, Committee Member



Dr. Choi, Hyun-Kyun, Committee Member

Department of Electrical, Electronic
and Computer Engineering,
University of Ulsan, Republic of Korea

July 2024

Copyright ©2024 – Yangde Gao

All rights reserved

VITA

Yangde Gao was born in Bengbu, China, in 1987. He completed his B.Sc. in Mechanical Design and Manufacturing and Automation in 2012 from Anhui Science and Technology University, Anhui, China. He completed his M.Sc. in Mechatronic Engineering in 2018 from Shanghai University of Engineering Science, Shanghai, China. After graduation, he joined as an engineer at the Shanghai Advanced Research Institute, Chinese Academy of Sciences. Since March 2021, he has been working on his Ph.D. Degree in the Department of Electrical, Electronic, and Computer Engineering, University of Ulsan, South Korea, under the supervision of Professor Jong-Myon Kim. His Ph.D. dissertation focuses on artificial intelligence techniques for rolling element bearings fault diagnosis. His current research interests include Machine learning, deep learning, artificial intelligence for energy, and industrial data analysis, such as machine condition monitoring, image classification, and pipeline leak localization.

Dedicated

... to Professor

... to my mother, who always wished me for this achievement

... to my father, for his countless prayers and endless support

...to my classmates, for their support and understanding.

ACKNOWLEDGEMENTS

Firstly, I'd like to express my deepest gratitude to my advisor Prof. Jong Myon Kim for his kind supervision and continuous support for my PhD study and associated research work, as well as his patience, encouragement, and tremendous knowledge. Throughout my PhD, he has provided me with excellent technical and non-technical assistance. Without his help, the vision of both the study and the research would be fuzzy. I am grateful for his guidance, advice, and generous support during my education. In addition to my advisor, I also extend my thanks to my Ph.D. supervisory committee for investing their time in the advancement of my thesis

I want to express my gratitude to my parents who supported me morally and financially throughout my life, as well as to my best friends who always stood by me in any circumstances and encouraged me psychologically. I am grateful to all of my fellow lab members in the Ulsan Industrial Artificial Intelligence Laboratory (UIAI LAB) at the University of Ulsan (UoU) for their assistance during my study.

I would also like to gratefully acknowledge the financial support of the BK21 plus program, the Korea Institute of Energy Technology Evaluation and Planning (KETEP), the Ministry of Trade, Industry & Energy (MOTIE) of the Republic of Korea, the Ministry of Science, ICT and Future Planning, and the National Research Foundation of Korea (NRF). Additionally, I am thankful to the University of Ulsan for his support.

Yangde Gao

University of Ulsan, Ulsan, Republic of Korea

July 2024

ABSTRACT

In modern industries, rolling element bearings are extensively utilized in complex mechanical fields that operate under severe conditions. Consequently, various failures may occur over extended periods of operation. Fault diagnosis employs various methods to ensure safe operation and minimize losses in rolling element bearings, which is especially important. Fault diagnosis encompasses signal acquisition, feature extraction, fault classification, and fault recognition. Fault classification involves categorizing the types of faults that occur in rolling element bearings, artificial intelligence (AI) techniques can detect most intrinsic mechanical information and identify fault features for rolling element bearings. Additionally, to continuously monitor the health conditions of rolling element bearings over time, numerous prognostic approaches are available to analyze diverse features derived from degradation data and assess the health conditions of rolling element bearings. AI techniques are popularly employed to predict the remaining useful life (RUL) of rolling element bearings, thereby facilitating effective prognostics and health management (PHM) of these components. Given the shared data, sequential relationships, and integrated approach characteristics, so, Fault classification and RUL prediction emerge as the primary focuses in the field of fault diagnosis for rolling element bearings, artificial intelligence techniques are proposed for fault diagnosis purposes on rolling element bearings.

Firstly, we propose a novel hybrid deep learning method (NHDLM) for fault classification in rolling element bearings. This method combines Extended Deep Convolutional Neural Networks with Wide First-layer Kernels (EWDCNN) and long short-term memory (LSTM). The EWDCNN method extends the convolution layers of WDCNN, enhancing automatic feature extraction. Subsequently, the LSTM then modifies the geometric architecture of the EWDCNN, resulting in a novel hybrid method (NHDLM), which further enhances the feature classification performance. The proposed NHDLM method demonstrates superior performance in the fault classification for rolling element bearings.

Secondly, to enhance prognostics and health management (PHM) for rolling element bearings, this paper proposes an efficient approach based on adaptive maximum second-order cyclostationarity blind deconvolution (ACYCBD) and a convolutional LSTM autoencoder. This approach aims to achieve feature extraction, health index analysis, and RUL prediction for

rolling element bearings. The ACYCBD is utilized to filter noise signals from vibration signals. A novel health index (HI) is designed based on peak value properties to analyze health conditions for the denoised signal. Then, employing convolutional layers and LSTM, the autoencoder transforms into a convolutional LSTM autoencoder (ALSTM) model, which is applied to forecast the trend for rolling element bearings. Compared with SVM, CNN, LSTM, GRU, and DTGRU methods, the proposed approach demonstrates superior performance in predicting the remaining useful life of rolling element bearings.

Finally, to enhance the prediction of RUL for rolling element bearings, a new optimal adaptive maximum second-order cyclostationarity blind deconvolution (OACYCBD) is developed for denoising vibration signals obtained from rolling element bearings. This method builds upon the traditional adaptive maximum second-order cyclostationarity blind deconvolution (ACYCBD) through optimization. To optimize the weights of conventional ACYCBD, the proposed method utilizes a probability density function (PDF) of Monte Carlo to assess fault-related incipient changes with the vibration signal, Cross-entropy is employed as a convergence criterion for denoising. In the subsequent step, a novel health index is calculated using the peak value and the square of the arithmetic mean of the signal. A newly developed hybrid invertible neural network (HINN) combines an invertible neural network and long short-term memory (LSTM) to forecast trends in rolling element bearings. The proposed approach outperforms existing methods in predicting the remaining useful life of rolling element bearings. These advancements pave the way for effective prognostics health management (PHM) through fault classification and RUL prediction for rolling element bearings.

Contents

VITA	vi
ACKNOWLEDGEMENTS	viii
ABSTRACT.....	viii
Contents.....	x
List of Figures.....	xii
List of Tables	xiii
Nomenclature.....	xiv
Chapter 1 Introduction.....	1
1.1. Background Information.....	1
1.2. Motivation	3
1.3. Thesis Objectives and Contributions	5
1.4. Thesis Outline.....	6
Chapter 2 Dataset Description.....	8
2.1. Case Western Reserve University (CWRU).....	8
2.2. Intelligent Maintenance System (IMS) Data	9
Chapter 3 A Novel Hybrid Deep Learning Method For Fault Diagnosis of Rolling Element Bearings Based on Extended WDCNN and Long Short-Term Memory	11
3.1. Introduction.....	11
3.2. Technical Background	13
3.2.1. WDCNN Model.....	13
3.2.2. Long Short-Term Memory	15
3.3. Methodology.....	17
3.4. Experimental results	18
3.5. Conclusions.....	28
Chapter 4 The Prediction of the Remaining Useful Life of Rolling Element Bearings Based on Using an Optimal Blind Deconvolution Method and Novel Deep Learning Methods.....	29
4.1. Introduction.....	29
4.2. Technical Background	34
4.2.1. ACYCBD method.....	34
4.2.2. OACYCBD method.....	40
4.2.3. Convolutional LSTM autoencoder.....	47
4.2.4. The Hybrid Invertible Neural Network.....	49
4.3. Methodology.....	51
4.3.1. ACYCBD and Convolutional LSTM autoencoder for RUL prediction	51
4.3.2. The OACYCBD and Hybrid Invertible Neural Network for RUL prediction	52

4.4. Experimental Results.....	53
4.4.1. The experiment 1	54
4.4.2. The experiment 2.....	56
4.5. Conclusions.....	61
Chapter 5 Summary of Contributions and Future Work.....	64
5.1. Summary of Contributions.....	64
5.2. Future work.....	65
Publications.....	66
References	68

List of Figures

Figure 2.1. Vibration bearing system used by CWRU.	9
Figure 2.2. Bearing platform on bearing degradation.....	10
Figure 3.1. Architecture of the WDCNN model.	15
Figure 3.2. The Long Short-Term Memory information.	16
Figure 3.3. Architecture of the proposed NHDLM model.....	17
Figure 3.4. The Fault Classification framework of the proposed NHDLM method.	18
Figure 3.5. vibration signatures of bearing fault.	19
Figure 3.6. Feature visualization via t-SNE: feature representation for ten fault styles of vibration signals extracted from 6 convolutional layers and 2 LSTM networks.	22
Figure 3.7. Confusion matrixes of different models.....	23
Figure 3.8. Evaluation indexes of different models.....	24
Figure 4.1. Flowchart of the ACYCBD method.	37
Figure 4.2. The raw vibration signals: (a) signals information in the time domain;	38
Figure 4.3. Results obtained by ACYCBD: (a) the denoising signal in the time domain; (b) frequency-amplitude on envelope spectrum.	39
Figure 4.4. The density distribution of a Monte Carlo simulation using a random variable..	41
Figure 4.5. Flowchart of the proposed OACYCBD.	43
Figure 4.6. Raw vibration signals.	44
Figure 4.7. Results from ACYCBD: (a) denoised signal in the time domain; (b) envelope spectrum.	44
Figure 4.8. Results obtained from OACYCBD: (a) the denoised signal; (b) envelope spectrum.	45
Figure 4.9. The peak signal theory.....	46
Figure 4.10. The LSTM constituted element.	47
Figure 4.11. Illustration of the convolutional LSTM autoencoder.	48
Figure 4.12. An invertible neural network.....	50
Figure 4.13. An illustration of the proposed hybrid invertible neural network.	51
Figure 4.14. The proposed prognosis framework for whole approach processing.	52
Figure 4.15. The proposed prognosis framework.....	53
Figure 4.16. The proposed approach for the whole verified experiment: (a) raw and denoised signals, (b) RMS and HI analysis, (c) convolutional LSTM autoencoder prediction model.	54
Figure 4.17. The proposed approach for the whole verified experiment: (a) raw and denoising signals, (b) RMS and health index analysis, (c) convolutional LSTM autoencoder prediction model.....	55
Figure 4.18. The proposed approach for the whole verified experiment: (a) raw and denoising signals, (b) RMS and health index analysis, (c) convolutional LSTM autoencoder prediction model.....	55
Figure 4.19. Bearing degradation processing results using different methods: (a) filtered signal by OACYCBD, (b) health index trend, and (c) forecast model using a hybrid INN model.....	57
Figure 4.20. The processing for different methods on bearing degradation: (a) denoised signal by OACYCBD, (b) health index trend of bearing degradation, and (c) forecast model using a hybrid INN model.....	58
Figure 4.21. Processing for different methods for bearing degradation: (a) filtered signal by OACYCBD, (b) health index trend of bearing degradation, and (c) a forecast model on hybrid INN model.	58
Figure 4.22. Performance comparison of model prediction.....	59

List of Tables

Table 2.1 Datasets for vibration bearing fault diagnosis.....	9
Table 3.1. Details of the proposed novel hybrid DL method used in the experiment.	20
Table 3.2. Prediction precision for different models.	26
Table 3.3. Prediction precision for comparison under the same conditions.	27
Table 3.4. The classification accuracy and time consumption.	27
Table 4.1. Parameters for the ALSTM architecture.	48
Table 4.2. Method prediction comparison.....	55
Table 4.3. Performance comparison of model prediction.	59

Nomenclature

AI	Artificial Intelligence
ANN	Artificial Neural Networks
CNN	Convolutional Neural Network
ML	Machine Learning
SVM	Support Vector Machine
WT	Wavelet Transform
EMD	Empirical Mode Decomposition
DL	Deep learning
WDCNN	Deep Convolutional Neural Networks with Wide First-layer Kernels
Conv Layer	Convolution Layer
LSTM	Long Short-Term Memory
KNN	K-Nearest Neighbor
PL	Pooling Layer
RNN	Recurrent Neural Network
BF	Ball Fault
IF	Inner Race Fault
OF	Out Race Fault
t-SNE	T-Distributed Stochastic Neighbor Embedding
1-D	One Dimensional
2-D	Two Dimensional
MSE	Mean Squared Error
RMSE	Root-Mean-Square Error
SNR	Signal-To-Noise Ratio
ACYCBD	Adaptive Maximum Second-Order Cyclostationarity Blind Deconvolution
PDF	Probability Density Function
MCKD	Maximum Correlated Kurtosis Deconvolution
MOMEDA	Multipoint Optimal Minimum Entropy Deconvolution

CYCBD	Maximum Second-Order Cyclostationarity Blind Deconvolution
PHM	Prognostics And Health Management
RUL	Remaining Useful Life
NHDLM	A Novel Hybrid Deep Learning Method
EWDCNN	Extended Deep Convolutional Neural Networks with Wide First-layer Kernels
INN	Invertible Neural Network
OACYCBD	Optimal Adaptive Maximum Second-Order Cyclostationary Blind Deconvolution
HINN	Hybrid Invertible Neural Network
HI	Health Index
ALSTM	Convolutional LSTM Autoencoder
IMS	Intelligent Maintenance System
GRU	Gated Recurrent Unit
DTGRU	Dual-Thread GRU

Chapter 1 Introduction

Rolling element bearings are used in many mechanical systems, such as engines, transport vehicles, and industrial machinery. Commonly utilized in extreme industries under heavy pressures and speed conditions. As a result, numerous failures may occur over running time, which damages the economics of the industries, so the protection of rolling element bearings is becoming more and more important. Fault diagnosis employs a variety of techniques to assure safe operation and minimize losses for rolling element bearings, which is especially critical [1-3]. Fault diagnosis includes data collection, feature extraction, fault classification, and fault recognition. Fault classification can identify the sorts of defects that occur in rolling element bearings. Artificial intelligence approaches can detect most of the intrinsic mechanical information and identify fault characteristics [4-6]. Meanwhile, sensors are employed to gather degradation data from rolling element bearings to detect faults, and several prognostic techniques are available to analyze various aspects resulting from degradation data and estimate health status. Artificial intelligence algorithms are used to forecast the remaining useful life (RUL) of rolling element bearing. This method may efficiently accomplish prognostics and health management (PHM) for rotating machinery [7-9]. So, Fault classification and remaining useful life (RUL) prediction are important aspects in the field of fault diagnosis for rolling element bearings. Artificial intelligence algorithms are proposed for fault diagnosis on rolling element bearings.

1.1. Background Information

In recent years, several machine-learning methods have been created for fault diagnosis on rolling element bearings. The support vector machine (SVM) has the benefit of a globally optimal solution that can be widely applied to classification in fault diagnosis, however, SVM is a shallow model and cannot immediately perform self-learning features from vibration signal obtained from rolling element bearings [10, 11].

Compared with typical machine learning approaches, deep learning (DL) can handle multiple nonlinear processing layers, it can make use of self-learning to automatically extract features from vibration signals, and deep learning methods are very popular in many research fields [12-14]. Convolutional neural networks (CNNs) are used to extract important features from vibration signals [10]. Deep convolutional neural networks (DCNNs) are presented to improve reinforced learning of vibration features, which can reuse weights and have better performance than traditional CNN [14]. the WDCNN model is proposed for better

performance of extraction features on vibration signals [12]. However, when considering a complex condition, it still requires a large amount of data for training and decreases rapidly. Although complex DL models can perform well for rolling element bearings diagnosis, they still require a lot of computational time and training examples. To address these problems, it is necessary to develop a novel hybrid deep learning approach to improve the fault classification performance of vibration signals.

After addressing fault classification for rolling element bearings, to make sure how long the element can be used as the next problem, over several years, various effective PHM measures have been developed to assess the health state of rolling element bearings researchers, after filtering processing, a health index was designed to show instant degradation and overall health conditions, and then deep learning method is applied to the prediction of the RUL of rolling element bearings, RUL prediction can enhance safety for element health management [8, 9]. In filtering parts, Minimum entropy deconvolution (MED) employs kurtosis maximization to differentiate weak impulse signals from rolling element bearings with noise signals, it still has issues and challenges with filter length and excessive kurtosis results [15]. To address these concerns and boost performance, maximum correlated kurtosis deconvolution (MCKD) improves the filtering performance through correlated kurtosis replacing kurtosis [16]. After that, Maximum second-order cyclostationarity blind deconvolution (CYCBD) iteratively resolves an eigenvalue problem to get the filtering coefficient and remove nosing signals, however, the CYCBD performance is therefore influenced by the prior cyclic frequency and filter length. To overcome these drawbacks, based on an autocorrelation function of a morphological envelope, adaptive maximum second-order cyclostationarity blind deconvolution (ACYCBD) has been developed to filter noise signals from vibration signals obtained from rolling element bearings [17, 18].

After filtering processing, support vector machines (SVMs) have effectively evaluated the state of rolling element bearings and analyzed convex optimization issues, SVM can employ both margin maximization and support vectors to achieve unambiguous separation in regression tasks [19, 20]. Except for machine learning methods, convolutional neural networks (CNNs) take advantage of several neural layers to represent feature values from input vibration signals and reduce higher numbers of dimensions, minimize the number of dimensions, and increase prognosis recognition [21-23]. However, CNNs suffer from overfitting, exploding gradients, and class imbalances, all of which degrade recognition performance. To improve the quality of a traditional CNN, a deep convolutional neural network (DCNN) was created to estimate the remaining usable life (RUL) of rolling element

bearings. These approaches can produce great prediction accuracy for predictions of the RUL of rolling element bearings. However, they often require their performance to be maintained under numerous assumptions and with large datasets [24-26]. To address prediction challenges, some novel methods are proposed for predicting the RUL of rolling element bearings. Experiments should demonstrate its effectiveness and superiority compared with existing methods.

1.2. Motivation

In the new paper, deep learning (DL) can make use of self-learning to automatically extract features from vibration signals, and deep learning methods are very popular in many research fields [27-29]. the WDCNN model is utilized to achieve better performance for fault classification however, when processing a complex large of data, it still consumes a large amount of time for training and testing, although complex deep learning models can achieve good results for classification, the process still consumes a lot of computational time and training samples [12]. Therefore, to address these issues, a novel hybrid deep learning method should be developed to improve the diagnosis performance of vibration signals. it is necessary to protect rolling element bearings.

Long short-term memory (LSTM) is designed for a novel memory architecture to address the gradient vanishing and exploding problem, making it suitable for prediction [29-30]. LSTM can also assist CNN in developing the CNN-LSTM, which has superior diagnostic ability. The CNN-LSTM architecture is designed to evaluate the vibration signals, when the CNN method has completed the feature extraction of one-dimensional singles, LSTM continues to process the critical features for fault classification [31-33]. LSTM can extract particular correlations for stronger automatic learning abilities of CNN in prediction, and these architectures provide numerous ideas that are relevant to this paper [34-36]. To address the above problems, the improved WDCNN method was merged with the LSTM method to create a novel hybrid method for fault classification of rolling element bearings.

After addressing fault classification for rolling element bearings, various effective deep learning approaches are designed to assess the health state and predict the remaining useful life of rolling element bearings, these methods are used for PHM measures. in these approaches, firstly, ACYCBD filtering is used to remove noise signals from vibration signals obtained from bearing degradation, after that, the health index is used for the instantaneous degradation and assessment of rolling element bearings for prognostics health management (PHM), to assess prognostic, Convolutional neural network (CNN) utilizes neural networks

to improve the prognostic recognition, CNN can automatically learn on remaining useful life (RUL) estimation for rolling element bearings, however, it has some disadvantages, such as overfitting and exploding gradients, which reduces the prediction performance [22-24]. To enhance prognostics and health management (PHM) for rolling element bearing degradation, LSTM can exploit the benefits of its design for preserving extended long memory for bearing degradation, LSTM can address limitations and overcome less stability for remaining useful life prediction, resulting in superiority forecasting [31, 32]. Because of the recurrent's native recurrence, LSTM involves sequential computing. This restricts the extent to which processes may be parallelized, potentially slowing training times.

To improve the quality of LSTM, a new model integrates the benefits of convolutional neural networks and LSTM to address RUL prediction limits for rolling element bearings, this method can extract sensing data to monitor health states, preserves these benefits, and overcomes overfitting of spatial fluctuations, resulting an efficient and accurate health monitoring. Meanwhile, several Autoencoder theories employ CNN and LSTM respectively for improving the prediction performance, these concepts are quite useful in this study [37-39]. To enhance the performance of the Convolutional LSTM method in the newest papers, combining convolutional layers with LSTM, autoencoder can transform convolutional LSTM to develop a convolutional LSTM autoencoder (ALSTM), this proposed method can achieve high prediction accuracy on RUL estimate of rolling element bearings.

In this research, ACYCBD has been effectively used for the diagnosis of rolling element bearings with cyclic frequencies. It can detect fault characteristics using the envelope harmonic product spectrum even without prior information. However, rolling element bearings may wear and tear under pressure and high-speed circumstances, and bearing deterioration can cause fault features at changeable cyclic frequencies [17, 18]. To maximize the adaptability of the ACYCBD method, the Monte Carlo probability density function (PDF) is employed to improve the filtering performance [40]. Cross-entropy replaces the conventional iteration process for ACYCBD, because these procedures optimize filter coefficients and enhance the filtering performance of vibration signals across a wide frequency range [41]. This approach enhances the use of ACYCBD in detecting bearing degeneration. Optimal adaptive maximum second-order cyclostationarity blind deconvolution (OACYCBD) is proposed for effectively filtering noise from signals related to bearing deterioration. OACYCBD performed very well in analyzing denoised signals resulting from bearing deterioration throughout a wide frequency range.

Following the successful filtering out of health-sensitive signals caused by the degradation of bearings, a health index was used to quickly assess the status of degradation and the overall health condition. The index is extremely important in assessing deterioration levels. It incorporates peak properties and the square of the arithmetic means to process denoised signals and analyze the bearing's health states [42]. It gives a time-domain measure of bearing deterioration that takes into account factors like pressure and speed, allowing it to show distinct phases of various health conditions under varied circumstances. It also exhibits greater susceptibility to rolling element bearing deterioration.

To improve PHM capabilities for bearing degradation prediction, the proposed method combines an INN with LSTM, resulting in a hybrid invertible neural network (HINN) that facilitates the mutual exchange of input features and outcome values and can seamlessly infer input features from given outcome values. This is consistent with the damage-accumulation mechanism seen in rolling element bearing degeneration [43-45]. By leveraging an invertible transformation, the HINN was meant to improve predicting performance by using an invertible transformation.

1.3. Thesis Objectives and Contributions

The primary objectives of this thesis are to develop effective artificial intelligence techniques for fault diagnosis of rolling element bearings, especially in bearings by combining feature extraction and artificial intelligence techniques. In this context, the contributions were made as follows:

Firstly, to address the aforementioned problems, the improved WDCNN method was merged with the LSTM method to create a novel hybrid approach for fault classification in rolling element bearings. The proposed approach makes use of reasonable neural networks and depth fusion of the LSTM network, and in each deep learning iteration, the model uses previous feedback and LSTM information to optimize extraction features and reduce the errors for fault classification. A novel hybrid deep learning method (NHDL) is presented that uses Extended Deep Convolutional Neural Networks with Wide First-layer Kernels (EWDCNN) and long short-term memory (LSTM) for complex environments. First, the EWDCNN method is proposed by expanding the convolution layer of WDCNN, which can increase automatic feature extraction. The LSTM then modifies the geometric architecture of the EWDCNN to design a novel hybrid method (NHDL), which can increase the performance of feature classification.

Secondly, the ACYCBD is used to separate noise signals from vibration signals. Second, using peak value properties, a novel health index (HI) is designed to examine the health status of the de-noising signal, resulting in a more sensitive capacity to detect bearing deterioration. Finally, to improve prognostics and health management for rolling element bearings, based on convolutional layers and LSTM, an autoencoder can achieve transform convolutional LSTM to create a convolutional LSTM autoencoder (ALSTM) model, which is used to forecast the trend for rolling element bearings. This proposed approach is designed to modify the convolutional recurrent nature of the network, resulting in excellent prediction accuracy for RUL estimates of rolling element bearings.

Finally, to better achieve RUL prediction for rolling element bearings, a new optimal adaptive maximum second-order cyclostationarity blind deconvolution (OACYCBD) is proposed to remove noise signals from vibration signals obtained from rolling element bearings. To optimize the coefficient weights of ACYCBD, a probability density function (PDF) of Monte Carlo is used to estimate trend changes in the bearing degradation, Cross-entropy replaces a convergence criterion for integration. A novel health index is calculated in the second step using the peak value and square of the arithmetic mean of the signal. To enhance PHM capabilities for bearing degradation prediction, this study combined an INN with LSTM, resulting in a hybrid invertible neural network (HINN). HINN is employed to forecast trends in rolling element bearings. All proposed approaches can achieve prognostics health management (PHM) through fault classification and RUL prediction for rolling element bearings.

1.4. Thesis Outline

The dissertation is composed of six major parts,

Chapter 1 briefly outlines the background information, motivations, objectives, and outline of the thesis.

Chapter 2 describes the acquisition platforms of the rolling element bearings utilized in this thesis.

Chapter 3 presents a novel hybrid deep learning method for fault diagnosis of rolling element bearings based on extended WDCNN and long short-term memory.

Chapter 4 The Prediction of the Remaining Useful Life of Rolling Element Bearings Based on Using an Optimal Blind Deconvolution Method and Novel Deep Learning Methods.

Chapter 5 summarizes the contributions and a discussion of future research directions.

Chapter 2

Dataset Description

In this dissertation, among the different signal types, we consider vibration-bearing current signals to demonstrate the results for every experimental analysis. Thus, the result analysis becomes consistent throughout the content. The current signal dataset used here is obtained from the Case Western Reserve University (CWRU) and the Intelligent Maintenance System (IMS). While considering the datasets, we have studied different load and speed conditions.

2.1. Case Western Reserve University (CWRU)

To validate this proposed method, public experimental bearing data from Case Western Reserve University (CWRU) were applied for fault classification, as shown in Figure 2.1 [12]. This experiment platform includes a transducer, dynamometer, and induction motor. The testing sampling frequency was 12 kHz, and in addition to the Normal Condition (NC), there were also three fault types of the vibration bearing: Ball Fault (BF), Inner Race Fault (IF), and Out Race Fault (OF). Each fault type has three levels of severity with fault diameters of 0.07 inches, 0.014 inches, and 0.021 inches, respectively. There were ten data styles of bearing health for training and testing: NC, BF7, BF14, BF21, IF7, IF14, IF21, OF7, OF14, and OF21. Each sample has 1024 points. Datasets A, B, C, and D respectively contain 700 training samples and 100 testing samples, 1400 training samples and 200 testing samples, 2100 training samples and 300 testing samples, and 2800 training samples and 400 testing samples of ten different fault conditions under loads of 0, 1, 2, and 3 hp. More details of the datasets are described in Table 2.1.

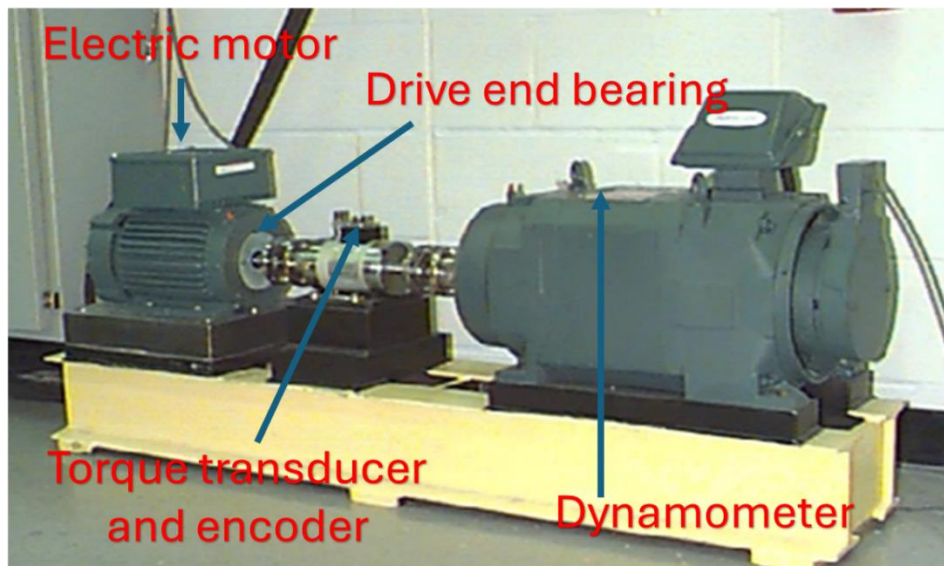


Figure 2.1. Vibration bearing system used by CWRU.

Table 2.1 Datasets for vibration bearing fault diagnosis.

Load (hp)	Fault Types	Fault Diameters	Training/Testing
0, 1, 2, 3	NC	0	'00/100, 1400/200, 2100/300, 2800/400
0, 1, 2, 3	BF	7	'00/100, 1400/200, 2100/300, 2800/400
0, 1, 2, 3	BF	14	'00/100, 1400/200, 2100/300, 2800/400
0, 1, 2, 3	BF	21	'00/100, 1400/200, 2100/300, 2800/400
0, 1, 2, 3	IF	7	'00/100, 1400/200, 2100/300, 2800/400
0, 1, 2, 3	IF	14	'00/100, 1400/200, 2100/300, 2800/400
0, 1, 2, 3	IF	21	'00/100, 1400/200, 2100/300, 2800/400
0, 1, 2, 3	OF	7	'00/100, 1400/200, 2100/300, 2800/400
0, 1, 2, 3	OF	14	'00/100, 1400/200, 2100/300, 2800/400
0, 1, 2, 3	OF	21	'00/100, 1400/200, 2100/300, 2800/400

2.2. Intelligent Maintenance System (IMS) Data

To validate the performance of the proposed prognostic approach, data from the Intelligent Maintenance System (IMS) center at the University of Cincinnati were used [21]. The

experiment involved four Rexnord ZA-21 15 double-row bearings. An AC motor operated at a constant speed of 2000 rpm and the data were sampled at 20,000 Hz. The applied load was 6000 foot pounds, and vibration data were monitored using PCB 353B33 High Sensitivity Quartz ICP accelerometers. The experimental platform in Figure 2.2 provides a basis for comparing the performance of various methods in the context of bearing degradation analysis.

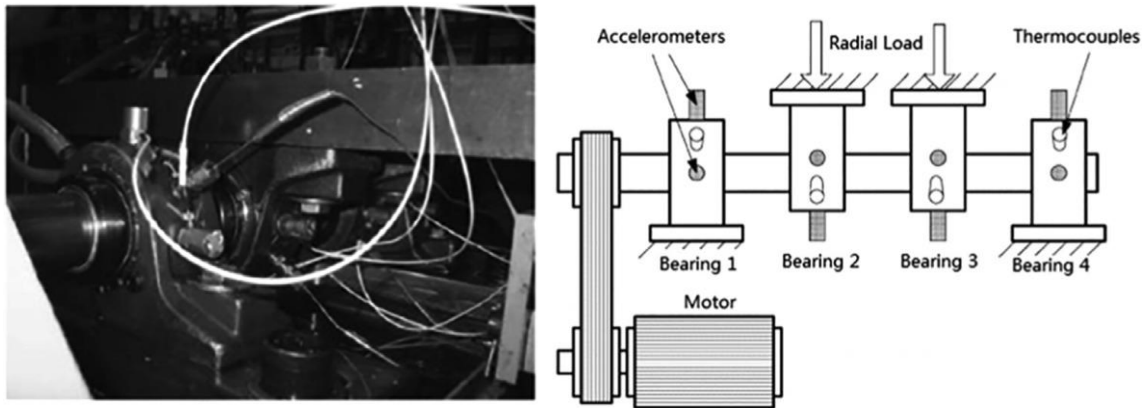


Figure 2.2. Bearing platform on bearing degradation.

Chapter 3

A Novel Hybrid Deep Learning Method For Fault Diagnosis of Rolling Element Bearings Based on Extended WDCNN and Long Short-Term Memory

3.1. Introduction

In modern industries, rotating machinery is widely used in complex mechanical fields that work under severe conditions. Therefore, various failures can occur over a long running time. Fault diagnosis uses various methods to ensure safe operation and reduce losses for rotating machinery, which is very important [46, 47]. Traditionally, fault diagnosis contains signal acquisition, feature extraction, and fault classification that can detect most intrinsic mechanical information and identify fault features [4-6]. There are a variety of fault diagnosis methods, including time-frequency analysis that can analyze the characteristic frequency of a vibration signal in the time domain; however, more time is required for data consumption. A wavelet transform (WT) was presented to filter noise and analyze features for vibration signals. Even so, WT still suffers some drawbacks when processing large amounts of non-linear vibration signals [15]. Empirical Mode Decomposition (EMD) was successfully applied to the fault diagnosis of the vibration signal; however, after extracting impulsive features from the vibration signals, the mode mixing problem remained [16].

In recent years, many methods based on machine learning have been developed for fault diagnosis. The support vector machine (SVM) has an advantage as a globally optimal solution that can be widely applied to classification in fault diagnosis; however, SVM is a shallow model and cannot immediately achieve feature self-learning from vibration signals [10, 11]. The k-nearest neighbor (KNN) method can achieve good performance for classification; however, it still has some difficulties for high-dimensional data [12]. Machine learning methods have achieved good performance in the classification of rotating machinery. However, their architecture still lacks multilayer non-linear mapping ability, and as a result, they cannot fully use previous information for classification, and existing methods need better performance for the amount of data in complex conditions [13-15].

Neural networks have the advantage of self-learning for fault prediction, and classification ELM has a simple structure and can achieve fast learning speed for higher prediction

performance. In addition, Artificial Neural Networks (ANNs) are used for fault diagnosis of vibration signals and the classification performance relies on the feature quality of vibration signals [29]. However, these methods still have inherent shortcomings. The parameters of similar approaches should be designed by humans before classifying features for vibration signals and they cannot guarantee their effectiveness on various optimal feature extraction. Additionally, when processing a massive dataset, they do not have very strong self-learning capability for complex classification.

Compared with traditional machine learning methods, deep learning (DL) can tackle multiple nonlinear processing layers, so it can automatically achieve self-learning and feature detection, which is very popular in many research fields. DL is based on modularized automatic learning network architectures; similarly, convolutional neural networks (CNN) are used to capture impact features of vibration signals [10]. Densely connected CNNs (DCNNs) are introduced to reinforce the collection learning of vibration features because of the weight reuse and better performance than traditional CNN [14]. the WDCNN model can achieve better performance for extraction features; however, when considering a complex condition, it still requires a large amount of data for training and decreases rapidly; although complex DL models can achieve good results for diagnosis, they still consume a lot of computational time and training examples [2, 12]. Therefore, to solve these problems, it is necessary to develop a novel hybrid DL method to improve the diagnosis performance of vibration signals.

Long short-term memory (LSTM) uses architecture to address the gradient vanishing and exploding problem, which can be used for prediction [29-30]. LSTM can also help CNN develop the CNN-LSTM, which has a stronger diagnostic ability. The CNN-LSTM network is constructed to analyze the vibration signals; when the CNN method finishes the feature of one-dimensional signals, LSTM continues to process this important information for diagnosis classification [31-33]. LSTM can extract special correlations for the stronger self-learning ability of CNN for prediction, and these architectures produce many ideas that are useful for this paper [34-36].

To address the above problems, the improved WDCNN method was combined with the LSTM method to produce a novel hybrid method for fault classification of rotating machinery. The proposed model uses the reasonable network structure and depth fusion of each neural network, and in each DL iteration, the model uses previous feedback and LSTM information to optimize extraction features and decrease the errors for fault classification.

The contributions of this paper are:

1. The novel hybrid DL method can be implemented under different bearing health conditions, which fully uses previous information for extraction features and has a stronger self-learning capacity to achieve high accuracy for fault classification.
2. The proposed method integrates the advantages of the improved WDCNN method and LSTM method, and uses various neural networks for stronger features of self-learning from large vibration signals.
3. t-SNE can show different mapping abilities of the neural networks for fault classification. This visualization can display how different layers capture the information step-by-step, and ten different fault styles of vibration-bearing signals were easily recognized by the novel hybrid DL method.

The rest of the paper is organized as follows. In Section 3.2, the basic theories of the WDCNN method and LSTM method are introduced, respectively. In Section 3.3, the improved WDCNN method and proposed framework of the novel hybrid deep learning method (NHDLM) are described in detail. In Section 3.4, experiments were performed to demonstrate different performances of the traditional CNN method, WDCNN method, EWDCNN method, and proposed method (NHDLM). The conclusions are presented in Section 3.5.

3.2. Technical Background

3.2.1. WDCNN Model

Feature To address the problems of the traditional CNN method, the WDCNN method was proposed for 1-D vibration signals under different conditions. The overall architecture contains convolutional layers, pooling layers, and one classification stage. Compared with the traditional CNN method, this architecture takes advantage of the first wide kernels to capture useful information from high-frequency noise signals, and then small kernels are used to acquire low-frequency features. The multilayer convolutional kernels make the networks deeper.

Convolutional Layer: in the convolutional layer, convolution operation was conducted on

the input local region with filter kernels/weight, and the output features were generated from input signals, input $x^l(j)$, convolution kernel K_i^l , and bias b_i^l of the i – the f filter kernel in layer l to produce an output feature map of the j – the l local region in layer l . The convolution process is described as follows:

$$y_i^{l+1}(j) = K_i^l * x^l(j) + b_i^l \quad (3.1)$$

where the $*$ notation computes the dot product of the kernel and local regions.

Activation Layer: After the convolution operation, a Rectified Linear Unit (ReLU) was used to enhance the representation ability and learned features for convolutional networks. As a useful activation unit, ReLU can adjust the parameters for training layers by weights, where $y_i^{l+1}(j)$ is the output value of the convolution operation. The formula is described as follows:

$$a_i^{l+1}(j) = f(y_i^{l+1}(j)) = \max\{0, y_i^{l+1}(j)\} \quad (3.2)$$

where $a_i^{l+1}(j)$ is the activation.

Pooling Layer: After the convolutional layer in the architecture, a max-pooling layer was used to reduce the spatial size of the features and parameters of a neuron in the previous layer, which performs the local max operation over the input feature map x_i and produces the output feature map y_i . The max-pooling layer is described as follows:

$$y_i = \max(x_i) \quad (3.3)$$

where the formula is a pooling operation for max-pooling and y_i denotes the corresponding value of the neuron.

Batch Normalization: After a convolutional layer or full-connected layer, the batch normalization (BN) layer is applied to reduce the shift of internal covariance, when input data is $x = (x^1, \dots, x^p)$, the BN layer is described as:

$$\hat{x}^i = \frac{x^i - E[x^i]}{\sqrt{Var[x^i]}}$$

$$y^i = \gamma^i \hat{x}^i + \beta^i \quad (3.4)$$

where γ^i is the scale parameter, β^i is shift parameter, and y^i is the output.

Architecture of the WDCNN Model: The overall architecture of WDCNN has filter stages and a classification stage as a traditional CNN model as shown in Figure 3.1. However,

the WDCNN model takes advantage of the first wide convolutional layer and multi-stage convolutional layers for stronger extraction features for input vibration signals. The WDCNN is used for 1-D input vibration signals without any other transformation, and multilayer small convolutional kernels can make the networks deeper to extract good representation. Batch normalization and a fully connected layer are then used to accelerate the training process.

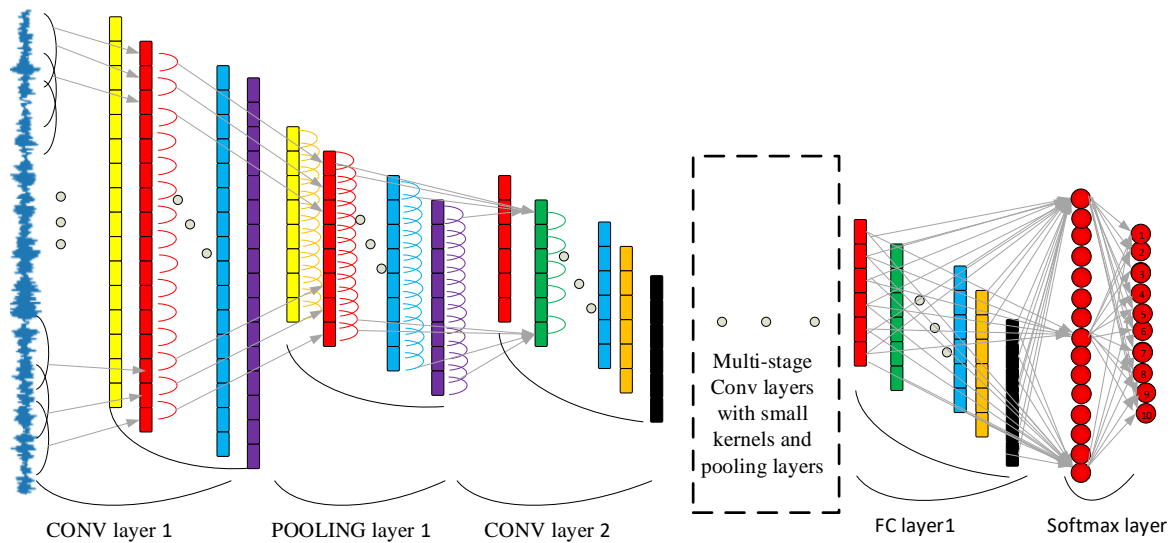


Figure 3.1. Architecture of the WDCNN model.

After extracting the features, the classification stage uses the fully connected layers for fault-style classification. For the output layer, the SoftMax function uses logits of ten neurons for the probability distribution of ten different bearing health conditions, described as:

$$q(z_j) = \frac{e^{z_j}}{\sum_k^{10} e^{z_k}} \quad (3.5)$$

where z_j is the logits of the j – th output neuron.

3.2.2. Long Short-Term Memory

As a modified version of a recurrent neural network (RNN), LSTM can take advantage of current and previous information on the current task and can address the drawback of traditional RNN for long-term memory. The LSTM network contains four gates, the forget gate, the update gate, the input gate, and the output gate. The LSTM method, as shown in Figure 3.2, can flexibly keep long-term memory of previous learning information, which means that the architecture of LSTM is more suitable for processing time series than RNNs.

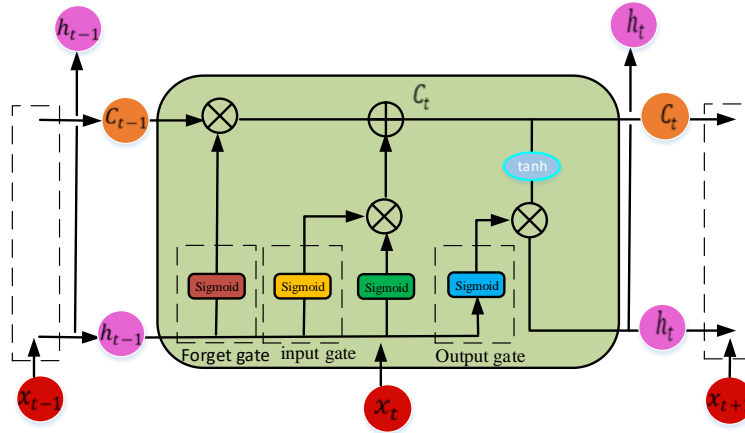


Figure 3.2. The Long Short-Term Memory information.

The forget gate was applied to capture important features from the previous neuron state in a one-layer neural network. The forget gate is described as follows:

$$f_t = \text{sigmoid}(W_f^T h_{t-1} + U_f^T x_t + b_f) \quad (3.6)$$

where x_t is the input vector at time t , h_{t-1} is the output of the memory block at time $t-1$, W_f^T , U_f^T are the weight vectors, and b_f is the bias vector. The input gate i_t can determine how much new information should be added to the current state of the neuron:

$$i_t = \text{sigmoid}(W_i^T h_{t-1} + U_i^T x_t + b_i) \quad (3.7)$$

The new memory content is calculated and updated as follows:

$$\tilde{C}_t = \tanh(W_c^T h_{t-1} + U_c^T x_t + b_c) \quad (3.8)$$

$$C_t = f_t * C_{t-1} + i_t * \tilde{C}_t \quad (3.9)$$

where C_t is the state information, \tilde{C}_t is the candidate state information, and \tanh is the hyperbolic tangent activation function. The output gate o_t is calculated to determine how much information should be used in the next time step:

$$o_t = \text{sigmoid}(W_o^T h_{t-1} + U_o^T x_t + b_o) \quad (3.10)$$

The output of the memory block is calculated as follows:

$$h_t = o_t \tanh(C_t) \quad (3.11)$$

In the architecture of LSTM, the memory unit C_t depends on the forget gate output f_t , the candidate memory information \tilde{C}_t , and the previous memory information C_{t-1} . The output h_t of the memory block depends on the output o_t of the output gate and value the

memory unit C_t .

3.3. Methodology

In this work, Before the proposed NHDLM method, the EWDCNN method was developed by extending the convolution layer of WDCNN. Convolutional layers were added to the architecture to develop the EWDCNN. Compared with the WDCNN model, the EWDCNN has six convolutional layers and results in a stronger deep learning capacity for signals. The architecture of EWDCNN was then exchanged with LSTM and the novel hybrid deep learning method (NHDLM) was developed, as shown in Figure 3.3. The architecture mainly consists of six convolutional layers with pooling layers, two LSTM, and one full connection layer.

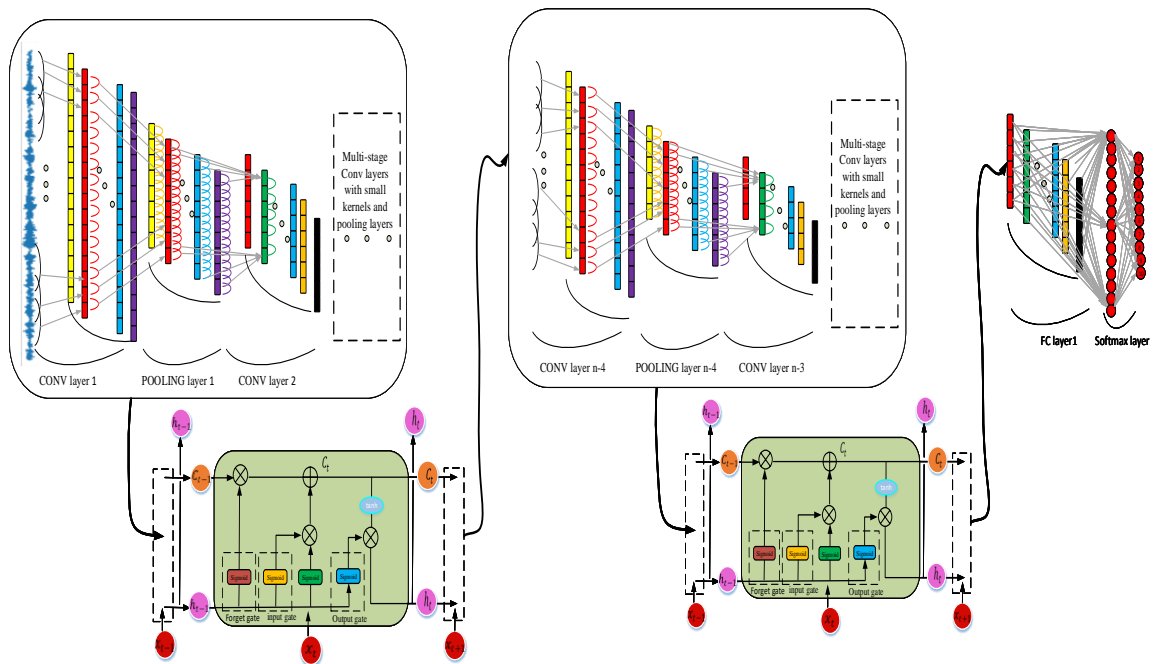


Figure 3.3. Architecture of the proposed NHDLM model.

The novel hybrid deep learning method is designed to extract the spatial and temporal variation features of 1-D vibration-bearing signals. The multiple convolutional layers can remove the noise from the vibration signals and extract the special features step-by-step. The proposed method based on two LSTMs can also take advantage of keeping the long short-term memory for extracting the time variation features of vibration signals and improving prediction. Finally, the full connection layer was used to integrate the feature information,

which was convenient for fault classification, realizing the nonlinear mapping, as shown in Figure 3.4.

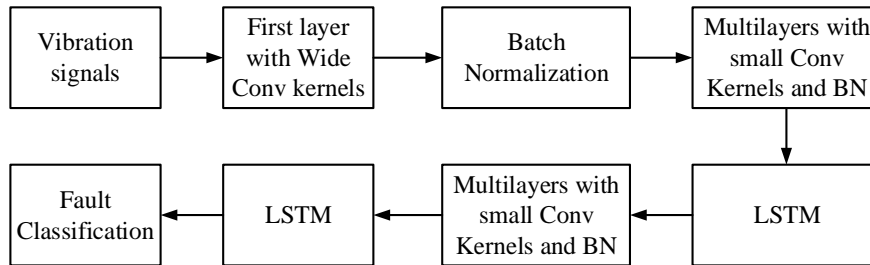
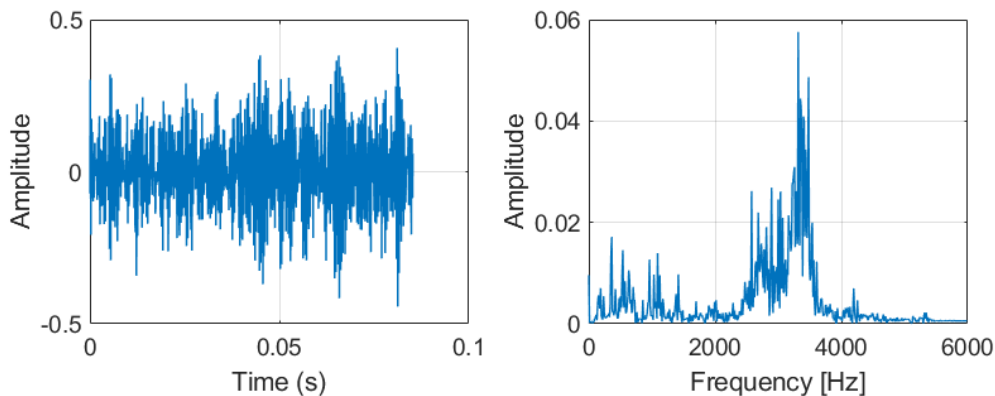


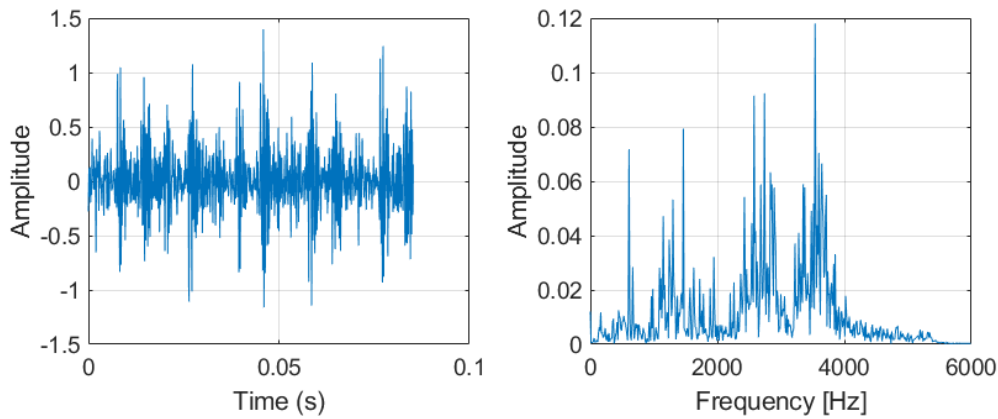
Figure 3.4. The Fault Classification framework of the proposed NHDLM method.

3.4. Experimental results

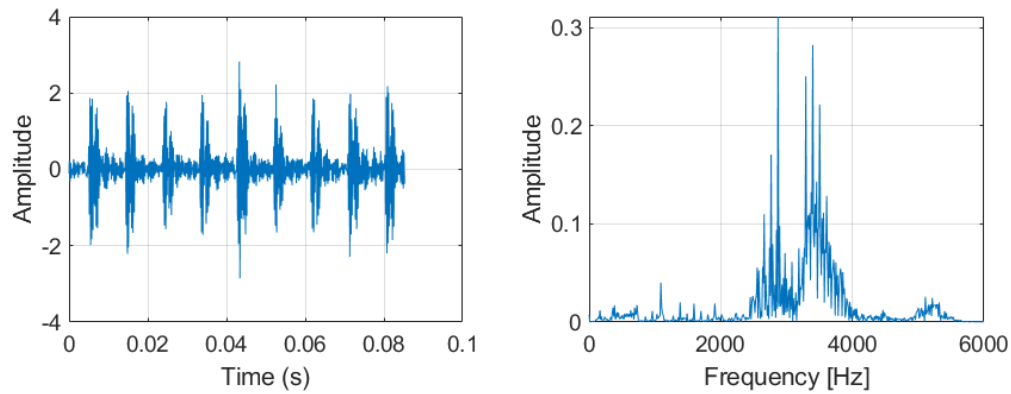
In this section, We also add vibration signatures of bearing fault in Figure 3.5. It is very difficult to diagnose Ball Fault (BF), many signals have impulsive content, and the ball fault is only engaging with the races in signals and is seemingly random. In the Inner Race Fault (IF), there are some strong harmonics, that with very clear impulsive modulation at shaft speed. Out Race Fault (OF) exhibits unnormal characteristic symptoms in the envelope spectra and has the most modulation at shaft speed.



(a) Ball Fault (BF) and Frequency.



(b) Inner Race Fault (IF) and Frequency.



(c) Out Race Fault (OF) and Frequency.

Figure 3.5. vibration signatures of bearing fault.

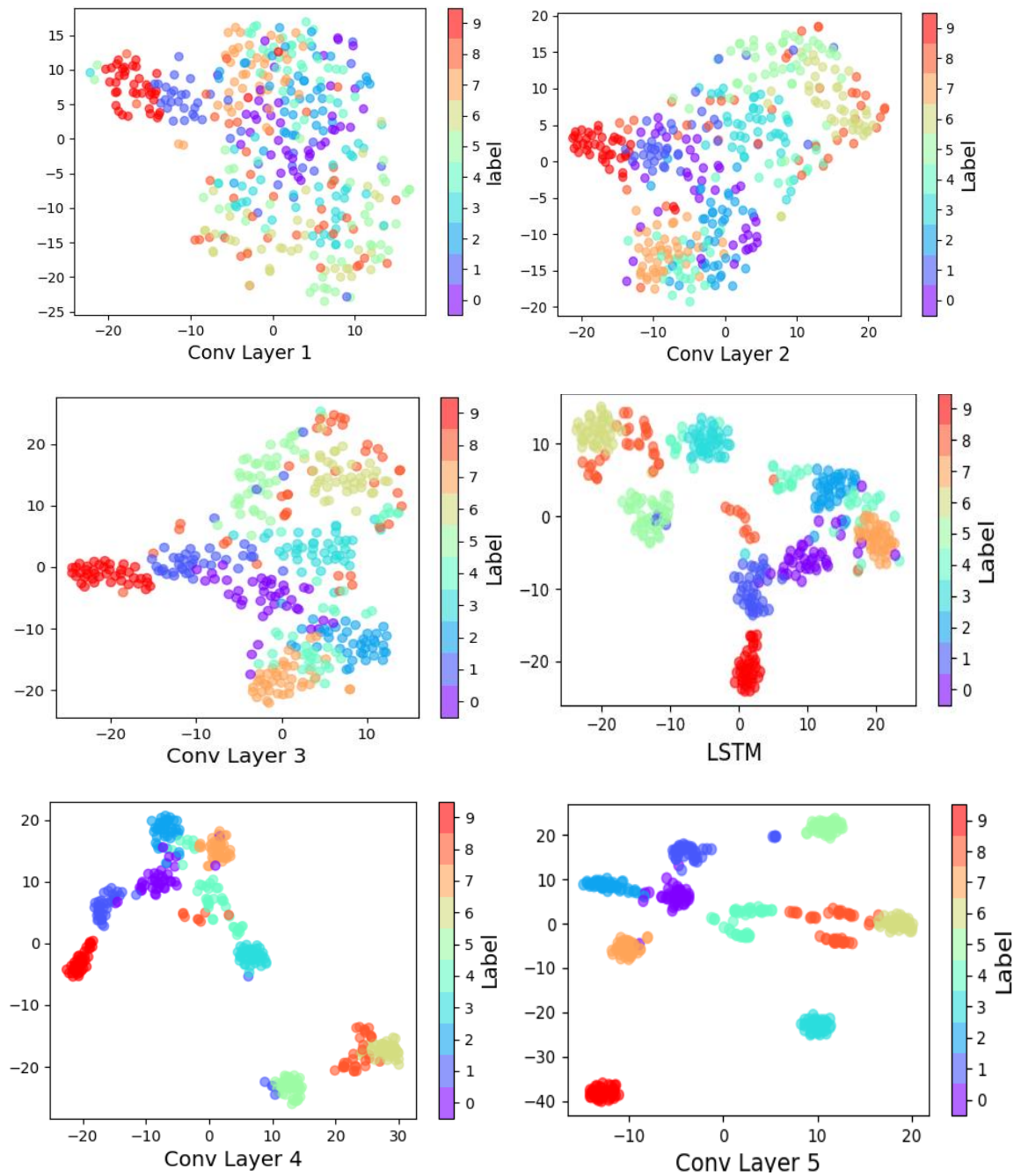
In this experiment, the architecture of the proposed novel hybrid DL method has 6 convolutional and pooling layers, 2 LSTM networks, fully connected hidden layers, and a soft-max layer. In this architecture, the size of the first convolutional kernel is $64 * 1$ and the rest of the kernel sizes are $3 * 1$. Max pooling is added after each convolutional layer, and then batch normalization is used to improve the performance of the method to select the adaptive size of the neuron. The parameters of the convolutional layers and LSTM network are detailed in Table 3.1, where Google TensorFlow and Python 3.7 were applied for the experiment.

Table 3.1. Details of the proposed novel hybrid DL method used in the experiment.

No.	Layer type	Kernel size	Kernel Number
1	Convolution1	64×1	16
2	Pooling1	2×1	16
3	Convolution2	3×1	32
4	Pooling2	2×1	32
5	Convolution3	3×1	64
6	Pooling3	2×1	64
7	LSTM	units=16	
8	Convolution4	3×1	64
9	Pooling4	2×1	64
10	Convolution5	3×1	64
11	Pooling5	2×1	64
12	Convolution6	3×1	64
13	Pooling6	2×1	64
14	LSTM	units=16	
15	Full-connected	100	1
16	SoftMax	10	1

According to feature visualization by mapping, the t-distributed Stochastic Neighbor Embedding (t-SNE) was applied to verify the self-learning feature capacity of the novel hybrid deep learning method under different neuro layers, as shown in Figure 3.6, which means ten fault styles of the vibration signals were easier to recognize. This visualization displays how different layers can capture information step-by-step using strong nonlinear mapping ability. All of the fault signals become separable and it does not perform very well in early layers; however, as the layer goes deeper, the model can make full use of the self-

learning capability for fault classification. The final layer finishes the cluster for ten fault styles of vibration-bearing signals.



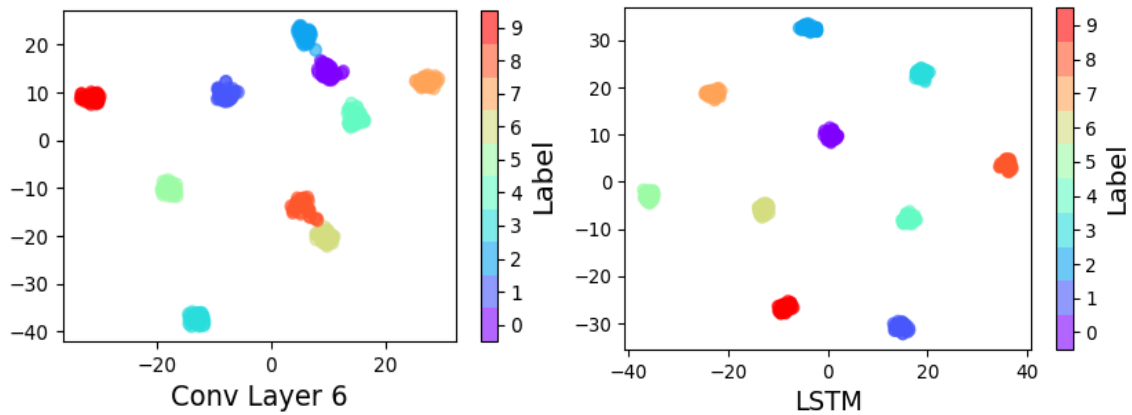
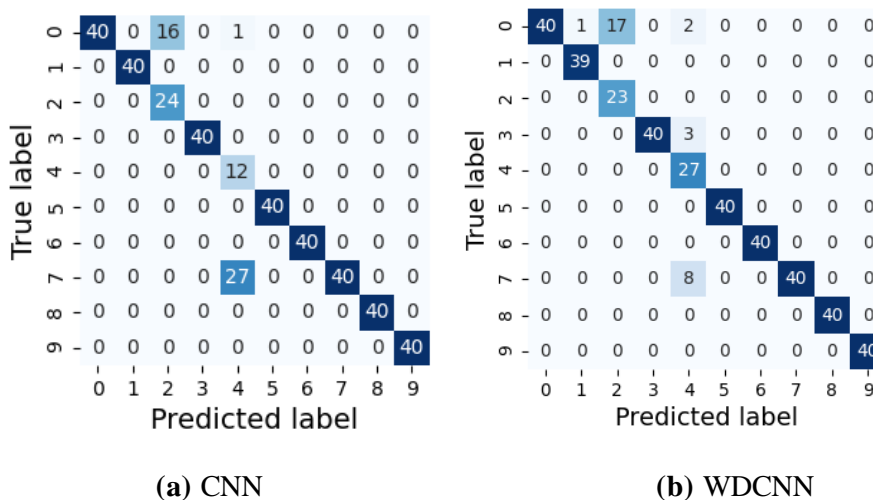


Figure 3.6. Feature visualization via t-SNE: feature representation for ten fault styles of vibration signals extracted from 6 convolutional layers and 2 LSTM networks.

As shown in Figure 3.7, there are approximately four confusion matrices for four predictive models (traditional CNN method, WDCNN method, improved EWDCNN method, proposed NHDLM method) trained on the 2800/400 train-test split. In each confusion, a blue rectangle means that all ten fault signals were correctly classified, a green rectangle means that the fault type was not classified correctly, and the number in a rectangle denotes the number of tests. For the first case (predictive model 1-traditional CNN), (400-43) out of 400 tests were correctly classified, which means that the traditional CNN hit an accuracy of 89% on sample testing. For predictive model 2 (WDCNN), (400-31) out of 400 tests were correctly classified for an accuracy of 92%. For predictive model 3 (EWDCNN), (400-11) out of 400 were correctly classified for a prediction accuracy of 97%. For the proposed method, (400-3) out of 400 were correctly classified for a classification accuracy hit of 99%. Many fault types were classified.



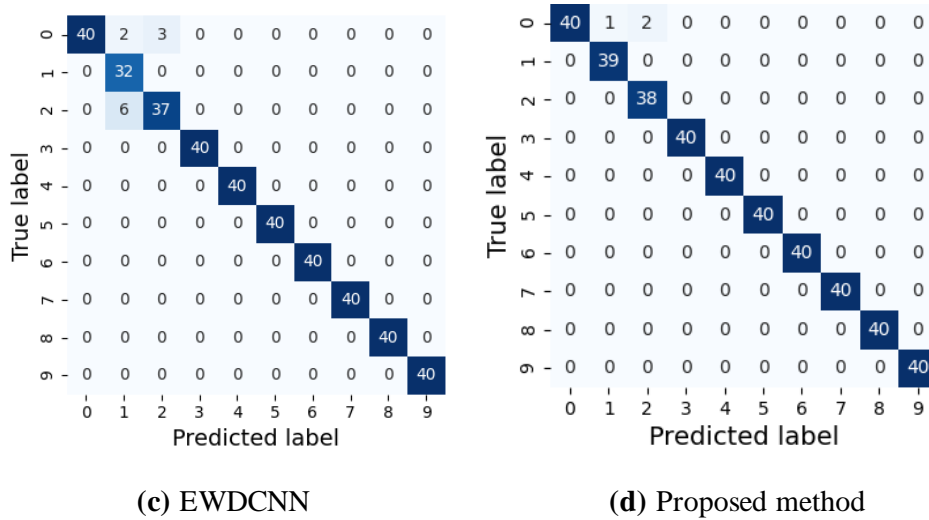


Figure 3.7. Confusion matrixes of different models.

To further verify the effectiveness of the proposed method in vibration signals, the A, B, C, and D datasets were applied to compare the CNN, WDCNN, and EWDCNN methods with the proposed NHDLM method. The simulation results are presented in Figure 3.8 and described below.

(a)Dataset A: For 700 training samples and 100 testing samples, the CNN approach achieved 50% prediction accuracy, the WDCNN method was 50%, the EWDCNN method was 51%, and the proposed NHDLM method was 58%. For 1400 training samples and 200 testing samples, the CNN approach achieved 73% prediction accuracy, the WDCNN method was 70%, the EWDCNN method was 71%, and the proposed NHDLM method was 81%. For 2100 training samples and 300 testing samples, the CNN approach achieved 76% prediction accuracy, the WDCNN method was 89%, the EWDCNN method was 92%, and the proposed NHDLM method was 96%. For 2800 training samples and 400 testing samples, the CNN approach achieved 89% prediction accuracy, the WDCNN method was 92%, the EWDCNN method was 97%, and the proposed NHDLM method was 99%.

(b)Dataset B: For 700 training samples and 100 testing samples, the CNN approach achieved 43% prediction accuracy, the WDCNN method was 50%, the EWDCNN method was 54%, and the proposed NHDLM method was 55%. For 1400 training samples and 200 testing samples, the CNN approach achieved 59% prediction accuracy, the WDCNN method was 64%, the EWDCNN method was 70%, and the proposed NHDLM method was 72%. For 2100 training samples and 300 testing samples, the CNN approach achieved 72% prediction accuracy, the WDCNN method was 92%, the EWDCNN method was 94%, and the proposed NHDLM method was 95%. For 2800 training samples and 400 testing samples, the CNN

approach achieved 87% prediction accuracy, the WDCNN method was 94%, the EWDCNN method was 96%, and the proposed NHDLM method was 98%.

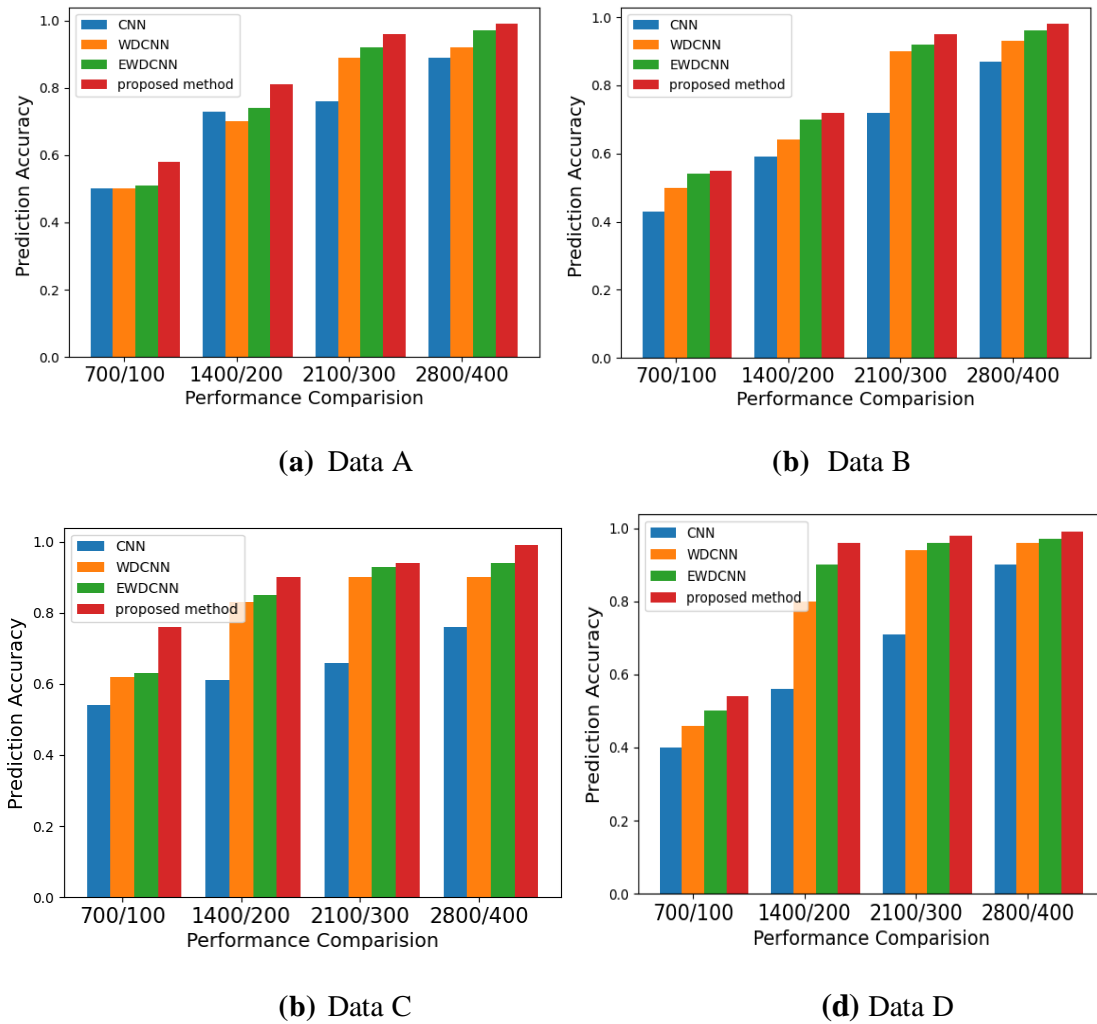


Figure 3.8. Evaluation indexes of different models.

(c) Dataset C: For 700 training samples and 100 testing samples, the CNN approach achieved 54% prediction accuracy, the WDCNN method was 62%, the EWDCNN method was 63%, and the proposed NHDLM method was 76%. For 1400 training samples and 200 testing samples, the CNN approach achieved 61% prediction accuracy, the WDCNN method was 83%, the EWDCNN method was 85%, and the proposed NHDLM method was 90%. For 2100 training samples and 300 testing samples, the CNN approach achieved 66% prediction accuracy, the WDCNN method was 90%, the EWDCNN method was 93%, and the proposed NHDLM method was 94%. For 2800 training samples and 400 testing samples, the CNN

approach achieved 87% prediction accuracy, the WDCNN method was 94%, the EWDCNN method was 97%, and the proposed NHDLM method was 99%.

(d)Dataset D: For 700 training samples and 100 testing samples, the CNN approach achieved 40% prediction accuracy, the WDCNN method was 46%, the EWDCNN method was 50%, and the proposed NHDLM method was 54%. For 1400 training samples and 200 testing samples, the CNN approach achieved 56% prediction accuracy, the WDCNN method was 80%, the EWDCNN method was 90%, and the proposed NHDLM method was 96%. For 2100 training samples and 300 testing samples, the CNN approach achieved 71% prediction accuracy, the WDCNN method was 94%, the EWDCNN method was 96%, and the proposed NHDLM method was 98%. For 2800 training samples and 400 testing samples, the CNN approach achieved 90%, the WDCNN method was 96%, the EWDCNN method was 97%, and the proposed NHDLM method was 99%.

The traditional CNN method still has some drawbacks for larger datasets, based on CNN, the WDCNN method can take advantage of the first wide convolutional layer and multi-stage convolutional layers for stronger extraction features. To enhance the self-learning capacity of the WDCNN method, the EWDCNN method is presented by extending the convolution layer of WDCNN, which can further improve automatic feature extraction. The LSTM then changes the geometric architecture of the EWDCNN to produce a novel hybrid method (NHDLM), which further improves the performance of feature classification. So, the proposed NHDLM method had the greatest identification accuracy for bearing datasets.

More information is shown in Table 3.2 to further illustrate the feasibility of the proposed method for different training and testing. When the training samples increased from 700 to 2800 and the testing sample increased from 100 to 400, the accuracy of these methods increased very obviously with the increasing samples. With 2800 training samples, the accuracy of the proposed method was greater than 99% and greater than the other methods. The proposed method had the greatest recognition accuracy in different datasets and methods, indicating promise for feature self-learning performance for vibration signals.

Table 3.2. Prediction precision for different models.

Data Set	Training/ Testing	CNN	WDCNN	EWDCNN	Proposed Method
A	700/100	0.5	0.5	0.51	0.58
	1400/200	0.73	0.7	0.71	0.81
	2100/300	0.76	0.89	0.92	0.96
	2800/400	0.89	0.92	0.97	0.99
B	700/100	0.43	0.5	0.54	0.55
	1400/200	0.59	0.64	0.7	0.72
	2100/300	0.72	0.92	0.94	0.95
	2800/400	0.87	0.94	0.96	0.98
C	700/100	0.54	0.62	0.63	0.76
	1400/200	0.61	0.83	0.85	0.9
	2100/300	0.66	0.9	0.93	0.94
	2800/400	0.87	0.94	0.97	0.99
D	700/100	0.4	0.46	0.5	0.54
	1400/200	0.56	0.8	0.9	0.96
	2100/300	0.71	0.94	0.96	0.98
	2800/400	0.9	0.96	0.97	0.99

Dataset E: we select data at the work speed of 1730 rpm, the load of 3HP, and fault diameter 0.021". For 1120 training samples and 160 testing samples, the WDCNN approach achieved 81% prediction accuracy, the EWDCNN method was 92%, and the proposed NHDLM method was 100%. For 2800 training samples and 400 testing samples, the WDCNN approach achieved 88% prediction accuracy, the EWDCNN method was 91%, and the proposed NHDLM method was 100%, as shown in Table 3.3.

Table 3.3. Prediction precision for comparison under the same conditions.

Data Set	Training/ Testing	WDCNN	EWDCNN	Proposed Method
E	1120/160	81%	92%	100%
	2800/400	88%	91%	100%

To further verify the effectiveness of the proposed method in training time, some datasets were applied to compare the CNN, WDCNN, and EWDCNN methods with the proposed NHDLM method. Training times are presented in Table 3.4. For 2800 training samples and 400 testing samples, the existing CNN, WDCNN, EWDCNN, and the proposed NHDLM require 14.595 seconds, 23.311 seconds, 22.166 seconds, and 30.636 seconds, respectively.

Table 3.4. The classification accuracy and time consumption.

Method	Time consumption	Overall Classification
(Training size/2800 samples)	(second)	Result (%)
CNN	14.595	87%
WDCNN	23.311	94%
EWDCNN	22.167	96%
NHDLM	30.636	98%

We also calculate some SNRs of training signals and testing signals, Ball Fault (BF): SNR= -2.3; Inner Race Fault (IF): SNR= -5.8; Out Race Fault (OF): SNR=-4.8; According to the datasets, the experiment can prove that the prediction accuracy can show the robustness of the proposed method.

3.5. Conclusions

In this paper, a novel hybrid DL method was proposed for fault classification for rotating machinery under complex working conditions. The health states contain different pressure loads, speeds, Fault Types, Fault Diameters, and training/testing samples. The proposed method was suitable for processing large datasets about vibration bearing signals and the method can achieve good performance for prediction.

Based on the WDCNN method, the EWDCNN method was developed by extending the convolution layer, and LSTM changes the EWDCNN's geometric architecture to develop the proposed NHDLM method. In the proposed NHDLM method, the architecture has different convolutional layers and LSTM networks. The LSTM networks can effectively increase the self-learning capability of the convolutional layers for ten fault styles of vibration signals, and the proposed model can effectively integrate the layer. The experiment proves that the proposed NHDLM method has a better performance than the existing CNN, WDCNN, and EWDCNN methods and NHDLM can achieve greater prediction accuracy on different fault styles of vibration signals.

The experiment proved that the proposed NHDLM method has better performance than the existing CNN, WDCNN, and EWDCNN methods, NHDLM can achieve greater prediction accuracy on different fault styles of vibration signals. Before deep learning methods process datasets, denoising preprocessing methods are not used. Therefore, some denoising methods can be used to preprocess and improve the performance of the deep learning methods in the future.

Chapter 4

The Prediction of the Remaining Useful Life of Rolling Element Bearings Based on Using an Optimal Blind Deconvolution Method and Novel Deep Learning Methods

4.1. Introduction

With the continued industrialization in society, rotating machinery is used in many fields, such as engines, transportation, and aircraft systems. Rotating machinery environments are severe and involve many reasons for failures. Sensors are used to collect data from rotating machinery, signal processing methods are deployed to remove noise, and deep learning methods are applied as prognostics to assess rotating machinery for health management (PHM) [48-52].

To assess prognostic and health management with good measures, based on margin maximization and support vectors, a support vector machine (SVM) is used to analyze the estimates of rotating machinery. However, there are some limitations, such as computation expense, model selection, and unsuitability for large datasets. To address these questions, a least square support vector machine (LSSVM) optimizes the health index to find a hyperplane for improving forecasting [48].

Except for machine learning methods, deep learning methods have been widely applied to prognostics for health monitoring in recent years. As a classic deep learning method, a convolutional neural network (CNN) utilizes the advantages of multiple neural layers to represent input data in feature values reduce higher numbers of dimensions and improve prognostic recognition [53–59]. However, CNNs suffer from overfitting, exploding gradients, and class imbalances that reduce recognition performance. To improve the quality of a traditional CNN, an optimal convolutional neural network was designed to estimate the remaining useful life (RUL) of bearings. Such networks effectively and simultaneously integrate global and local information, resulting in enhanced prediction performance [60-69]. Similar research, utilizing multi-source sensors, has shown that an improved deep CNN can

effectively extract data from multiple sensing sources for health-state monitoring. This approach retains the advantages of multi-source data while overcoming issues related to overfitting due to spatial fluctuations, ultimately leading to efficient and accurate health monitoring [70-73]. While these methods can achieve high prediction accuracy for estimates of the RUL of rotating machinery, they often require their performance to be maintained under numerous assumptions and with large datasets.

There are many prognostic approaches to analyzing health conditions for rotating machinery. Wavelet decomposition makes use of the time-frequency domain for analyzing machinery degradation, and minimum entropy deconvolution (MED) can use the maximum kurtosis to separate impulsive signatures for early-stage fault signals. However, MED needs to overcome excessive kurtosis [15, 74]. To resolve this, the maximum correlated kurtosis deconvolution (MCKD) is based on correlated kurtosis to improve filtering performance for vibration signals. From the cyclostationary view, MCKD does not have the best performance for statistical processing of signals [16]. Additionally, multipoint optimal minimum entropy deconvolution (MOMEDA) has been proposed, focusing on multipoint kurtosis. These methods excel at extracting impulse signals from mixed signals using an iteratively evaluated index [75–77]. From the cyclostationarity view, MCKD does not explicitly investigate its statistical nature, and MOMEDA is based on a periodic criterion to harness the power of cyclostationarity. By comparison, maximum second-order cyclostationarity blind deconvolution (CYCBD) can iteratively resolve an eigenvalue problem [78, 79]. As CYCBD can only amplify a fault signature with a specified cyclic frequency, the cyclic frequency needs to be determined in advance, and the ideal CYCBD performance is therefore influenced by prior cyclic frequency. In addition, filter length can affect CYCBD's denoising capabilities, with slight deviations leading to completely different results. To overcome these drawbacks, adaptive maximum second-order cyclostationarity blind deconvolution (ACYCBD) has been proposed to filter noise, based on an autocorrelation function of a morphological envelope. A cyclic frequency estimation is then applied in the architecture of ACYCBD while a search strategy is deployed to adaptively select the filter length and maintain a balance between performance and time costs when compared with CYCBD [80–82].

After filtering processing, a health index was used to assess instant degradation and overall health conditions before applying deep learning to the prediction of the RUL of rotating machinery to enhance safety. This index plays a pivotal role in tracking machinery

degradation. An effective health strategy can analyze critical equipment degradation and assess various health conditions. Given the complexity of degradation, designing an efficient health index that accurately represents machinery health states remains challenging and requires incorporating metrics such as the root mean square (RMS) and kurtosis. Subsequently, machine learning or deep learning techniques are used to predict the health conditions of the rotating machinery. This hybrid approach can effectively achieve prognostics and health management (PHM) of rotating machinery, even under varying operating conditions [83–87]. After successfully filtering out health-sensitive signals resulting from the degradation of bearings, a health index was applied to promptly assess the state of degradation and the overall health condition. The index plays a pivotal role in assessing degradation. It incorporates peak properties and the square of the arithmetic means to process denoised signals and analyze the health condition of the bearing. It provides a time-domain measure of bearing degradation, considering factors such as pressure and speed, allowing it to depict various health condition stages under different circumstances. It also exhibits greater sensitivity to bearing degradation.

To address data-related challenges, a transferable neural network method was used to predict the RUL of rotating machinery. This approach minimizes divergence in distance and conditional probability distributions to assess the health index, reducing reliance on the availability of high-quality data. The results demonstrate its effectiveness and superiority compared with existing methods [88–90].

For better prognostics and health management (PHM) for bearing degradation, LSTM can use the advantages of its architecture for long memory of bearing degradation and can address limits and problems for RUL prediction to achieve superior forecasting. Long short-term memory (LSTM) networks can use their architectural strengths to obtain long-term memories of bearing conditions. LSTM networks effectively address the limitations and instability issues associated with predicting the RUL of rolling bearings, producing superior forecasting performance [91–94]. The LSTM method demands greater memory to handle time sequences. LSTM involves sequential computations due to the recurrent nature of the network. This limits the extent to which operations can be parallelized, potentially slowing training times. To improve the quality of LSTMs, a new model integrates the advantages of CNN and LSTM to address limits for RUL prediction of rolling bearings. This method can extract sensing data to monitor health states, preserve these benefits, overcome overfitting of spatial fluctuations, and achieve efficient and accurate health monitoring [54-58]. In addition, some autoencoder

theories are applied to CNN and LSTM to improve prediction performance [59-61].

To improve the performance of the LSTM method and the Convolutional LSTM method application, based on convolutional layers and LSTM, autoencoders can achieve Transform Convolutional LSTM to develop a convolutional LSTM autoencoder (ALSTM). This proposed method is designed to transform the convolutional recurrent nature of the network and can achieve high prediction accuracy on RUL estimates of rotating machinery. The major contributions of this study are as follows.

In this paper, ACYCBD has been successfully applied to the detection of vibration-bearing faults characterized by cyclic frequencies. It can identify fault features using the envelope harmonic product spectrum, even without prior information. However, as machinery can experience wear and tear under pressure and high-speed conditions, bearing degradation can result in fault features at varying cyclic frequencies [17,18]. To enhance and optimize the adaptability of the ACYCBD method for such scenarios, we employed a Monte Carlo probability density function (PDF) [40]. We chose cross-entropy [41] to replace the conventional iteration process in ACYCBD as this modification optimizes filter coefficients and enhances the filtering performance of vibration signals across a wide range of frequencies. This approach further advances the application of ACYCBD in detecting bearing degradation. We proposed optimal adaptive maximum second-order cyclostationary blind deconvolution (OACYCBD) to effectively filter noise from signals associated with bearing degradation. OACYCBD proved particularly well-suited for analyzing denoised signals stemming from bearing degradation across a wide range of frequencies .

Bearing degradation, which is a measure of cumulative damage, implies that degradation in the next step is influenced by previous damage. This requires the ability to infer input features from given outcome values, resulting in mutual interference between input features and outcome values [95-99]. To address this challenge, an invertible neural network (INN) was designed to induce invertible transformation, which enables a mutual exchange between input features and outcome values, effectively harnessing the advantages of correlation information to enhance recognition performance. [43–45]. Bayesian optimization was used to enhance the performance of the INN. These concepts and strategies have proved to be highly beneficial [95,96].

To enhance PHM capabilities for bearing degradation, this study was designed to enhance bearing degradation prediction by integrating an INN with LSTM, resulting in a hybrid

invertible neural network (HINN) that facilitates the mutual exchange of input features and outcome values and can seamlessly infer input features from given outcome values. This aligns with the damage-accumulation process observed in bearing degradation. By leveraging an invertible transformation, the HINN was designed to optimize fore-casting performance.

1. ACYCBD is used to filter noise signals and to identify fault features for bearing degradation with cyclic frequency for vibrating signals. This method can avoid noise signal interference for bearing degradation, enhancing prognostic and health management under different operations. ACYCBD is successful for feature extraction regarding bearing degradation. Although ACYCBD excels at identifying fault features in vibration signals with cyclic frequencies, bearing degradation involves the accumulation of fault features at variable cyclic frequencies, particularly under high pressures and speeds. To enhance ACYCBD's filtering performance in this context, we introduced an OACYCBD method. In OACYCBD, we used a probability density function (PDF) of Monte Carlo to assess condition characteristics and detect subtle dissimilarities in vibration signals. We also replaced the traditional iteration process of ACYCBD with cross-entropy to optimize filter coefficients. These measures collectively led to a significant improvement in OACYCBD's ability to extract features from bearing degradation, surpassing the performance of ACYCBD, particularly when dealing with variable frequencies.

2. After filtering noise from bearing degradation signals, based on peak value properties, a good HI is designed to analyze key rotating machinery degradation and to measure health conditions in different situations. Once the noise signals stemming from bearing degradation have been filtered, the next step involves identifying peaks within the denoised signals and taking advantage of their peak properties. These peaks are then combined with the square of the arithmetic mean to produce a novel health index. A robust index is instrumental in analyzing critical aspects of equipment degradation and quantifying various stages of health conditions. We designed an index that evaluates bearing degradation across different pressure and speed scenarios in the time domain, thereby providing valuable insights into health conditions under diverse conditions.

3. To provide better prognostics for health management related to bearing degradation, based on convolutional layers and LSTM, an autoencoder can achieve Transform Convolutional LSTM to develop a Convolutional LSTM Autoencoder (ALSTM) with superior performance to the LSTM method. To enhance PHM capabilities for bearing degradation, we leveraged the strengths of both an INN and LSTM to create a HINN. The

HINN architecture allows for the mutual exchange of input features and outcome values. This unique characteristic gives the HINN the ability to effectively model the accumulation of damage during bearing degradation and outperform the LSTM method in terms of predictive performance.

The main content is described as follows. The ACYCBD and OACYCBD methods are described in Section 4.2. Convolutional LSTM Autoencode and hybrid invertible neural network are proposed in this section. In Section 4.3, two novel approaches are constructed. Experimental results and their discussions and conclusions are shown in Sections 4.4 and 4.5 respectively.

4.2. Technical Background

4.2.1. ACYCBD method

In the architecture of ACYCBD [17, 18], the envelope harmonic product spectrum (EHPS) can detect cyclic frequency in vibration signals for processing of CYCBD, as in the blind deconvolution theory. The input signal x is multiplied with the inverse FIR filter h to compute the source signal s_0 . The process is described as follows:

$$s = x * h = (s_0 * g) * h \approx s_0 \quad (4.1)$$

Here s is the estimated input, g is the impulse response, and the convolution operation is expressed as follows:

$$\begin{Bmatrix} s[L-1] \\ \vdots \\ s[N-1] \end{Bmatrix} = \begin{bmatrix} x[L-1] & \cdots & x[0] \\ \vdots & \ddots & \vdots \\ x[N-1] & \cdots & x[N-L-2] \end{bmatrix} \begin{Bmatrix} h[0] \\ \vdots \\ h[L-1] \end{Bmatrix} \quad (4.2)$$

where N represents the length of x , L denotes the length of the inverse FIR filter h , and the optimal inverse filter h_0 is described as follows:

$$h_0 = \underset{h}{\operatorname{arg\,max}} [O(h)] \quad (4.3)$$

Here $O(h)$ represents the objective function of the filtering processing, and a cyclic frequency is accumulated from the period of fault impact T_s , as follows:

$$\alpha = \frac{1}{T_s} \quad (4.4)$$

The key component assessment is described as second-order cyclo stationarity (ICS_2):

$$ICS_2 = \frac{\sum_{k>0} |c_s^k|^2}{|c_s^0|^2} \quad (4.5)$$

with

$$c_s^k = \langle |s|^2, e^{j2\pi k\alpha n} \rangle \quad (4.6)$$

$$c_s^0 = \frac{\|s\|^2}{N - L + 1} \quad (4.7)$$

ICS_2 is the objective function of the CYCBD:

$$h_0 = \arg \max_h ICS_2 \quad (4.8)$$

The Eigenvalue algorithm (EVA) is designed to optimize the filter coefficient for optimal filtering as follows:

$$c_s^k = \frac{EDs}{N - L + 1} \quad (4.9)$$

$$c_s^0 = \frac{s^H s}{N - L + 1} \quad (4.10)$$

with

$$D = \text{diag}(s) = \begin{bmatrix} \ddots & & 0 \\ & s[l] & \\ 0 & & \ddots \end{bmatrix} \quad (4.11)$$

$$E = [e_1 \cdots e_k \cdots e_K] \quad (4.12)$$

$$e_k = [e^{-j2\pi k\alpha(L-1)} \cdots e^{-j2\pi k\alpha(N-1)}]^T \quad (4.13)$$

The ICS_2 function is described as

$$ICS_2 = \frac{s^H D^H E E^H D s}{|s^H s|^2} \quad (4.14)$$

Finally, the result is calculated:

$$ICS_2 = \frac{h^H X^H W X h}{h^H X^H X h} = \frac{h^H R_{XWX} h}{h^H R_{XX} h} \quad (4.15)$$

Here R_{XWX} is the weighted correlation matrix, R_{XX} is the correlation matrix, and the weight matrix W is as follows:

$$W = \frac{D^H E E^H D}{S^H S} \quad (4.16)$$

λ is used to calculate the inverse filter h_0 equivalent to h as

$$R_{XWX}h = R_{XX}h\lambda \quad (4.17)$$

The architecture of ACYCBD is shown in Figure 4.1. The EHPS algorithm is applied to determine the cyclic frequency. The steps of the ACYCBD procedure are as follows.

Step 1: The filter length L , the initial filter coefficient h , the convergence criterion ε_0 , the maximum iteration number N_{max} , and the initial parameters are applied to compute the temporary signal s for the next optimal operation.

Step 2: The cyclic frequency is calculated using the EHPS method with the optimal maximum amplitude.

Step 3: According to the brief functions, we compute the weight matrix W , the correlation matrix R_{XX} , and the weighted correlation matrix R_{XWX} and optimize the filtering coefficient for achieving maximum eigenvalue operation.

Step 4: Repeat Step 2 with the updated value to calculate the optimal filtering coefficient h that satisfies the requirements of cyclic operation.

Step 5: Obtain the optimal denoising signals.

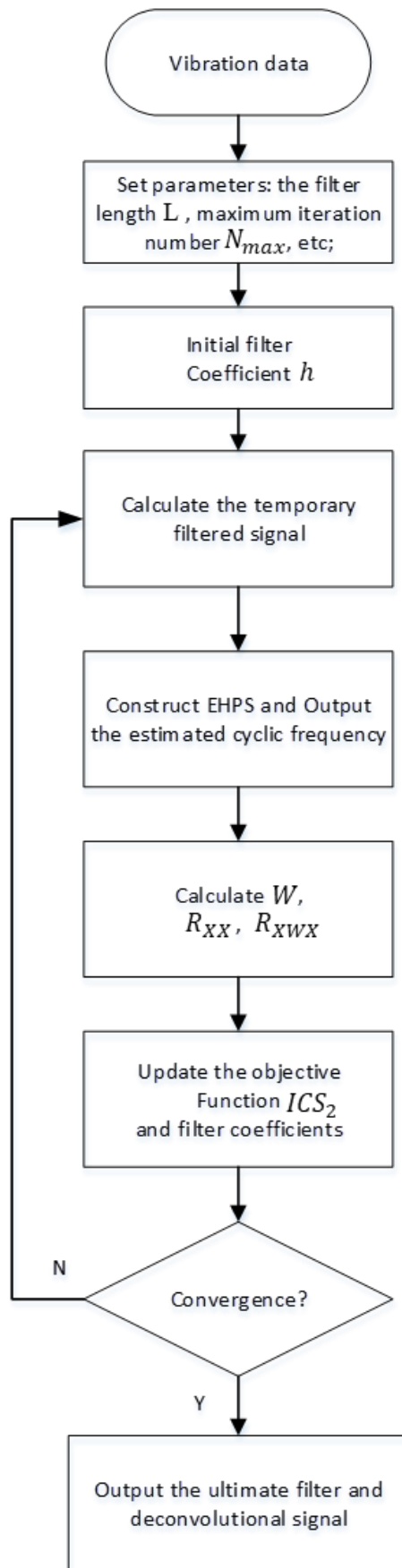


Figure 4.1. Flowchart of the ACYCBD method.

Vibration signals are applied to verify the performance of the ACYCBD method, as shown in Figure 4.2 and Figure 4.3. In the raw vibration signals, damage produces mixed signals including noise, which interferes with the performance analysis for vibration conditions.

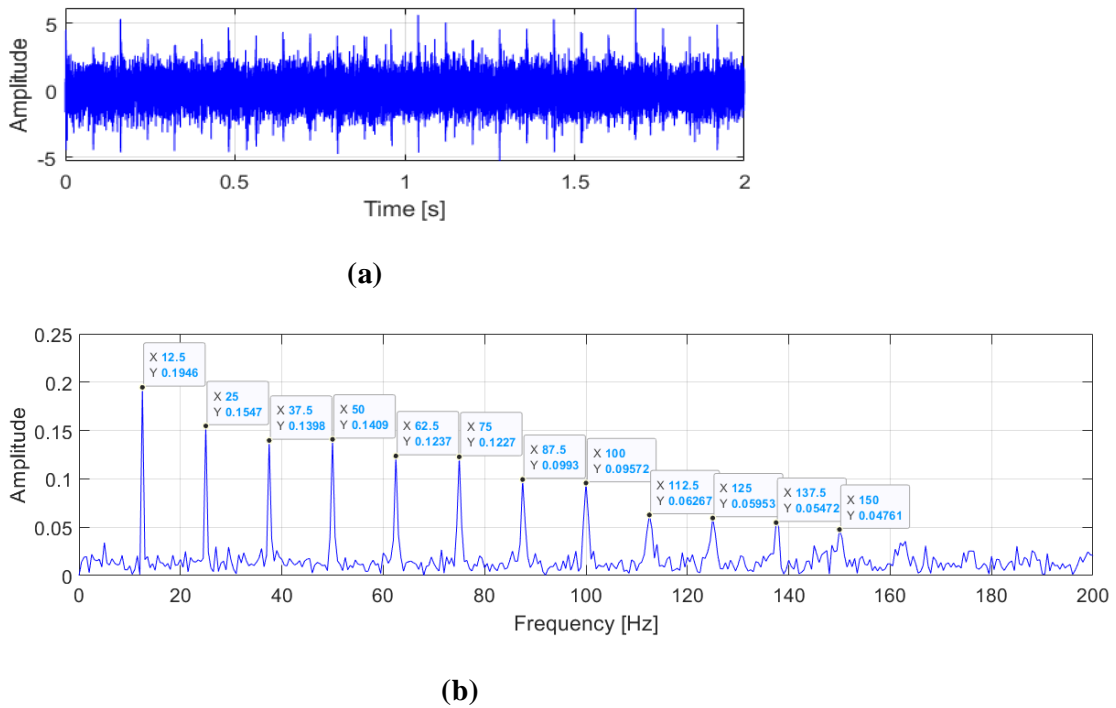
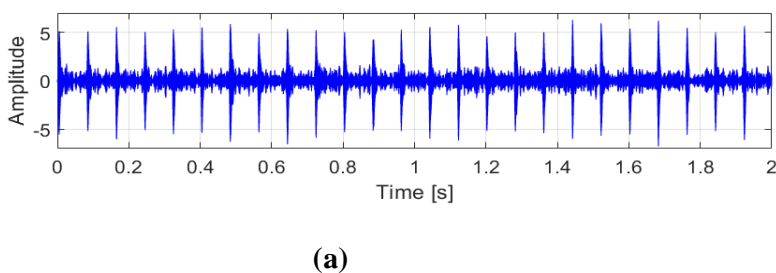
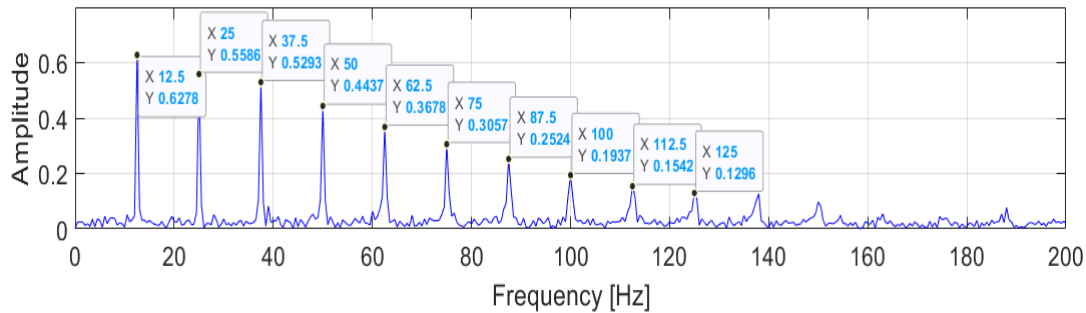


Figure 4.2. The raw vibration signals: (a) signals information in the time domain; (b) frequency-amplitude for envelope spectrum.





(b)

Figure 4.3. Results obtained by ACYCBD: (a) the denoising signal in the time domain; (b) frequency-amplitude on envelope spectrum.

The envelope spectrum of the raw signals is described in Figure 4.2. Fault frequency information is shown for analysis. The initial fault value is set at 12.5 Hz. The frequency multiplication can be calculated in the interval [12.5, 25, 37.5, 50, 62.5, 75, 87.5, 100, 112.5, 125...] Hz. There are distinct peaks at frequencies of 25, 37.5, and 50, which are close to two, three, and four times the frequency of a fault. In Figure 4.3, the ACYCBD filtering method is utilized to remove noise and to verify the effectiveness of the envelope spectrum. The result was obtained as a fault frequency of 12.5 Hz and was more obvious in ACYCBD processing. Frequency multiplication was extracted accurately, as [12.5, 25, 37.5, 50, 62.5, 75, 87.5, 100, 112.5, 125...] Hz, which shows that the distinct peak frequencies are 1-10 times higher than the 12.5 Hz fault frequency. At the same peak frequency of 12.5 Hz, the amplitude of the raw signal is 0.1946; for the ACYCBD, the amplitude is 0.6278. Other processes are also compared. The amplitude is greater than the raw vibration signals at the same peak frequencies, demonstrating the performance of ACYCBD filtering. The results show that the ACYCBD has good filtering performance for health analysis, as in the next step.

After filtering processing, to utilize deep learning methods for predicting bearing degradation, the HI is used for instantaneous assessment of degradation and health conditions. HI plays a vital role in the prediction of the degradation of machinery. A good HI strategy can analyze key components of equipment degradation for vibration bearings. In this study, the HI method is derived from the peak value theory. The maximum and minimum values are identified by analyzing the changes of the signal and the input vibration signals (x_1, \dots, x_n), searching the maximum and minimum values of n numbers from the

input data, calculating the difference values for maximum x_p and minimum x_q , and then evaluating the change from the input signals. The formula is as follows:

$$HI = x_p - x_q \quad (4.18)$$

4.2.2. OACYCBD method

ACYCBD has been successfully applied to the detection of vibration-bearing faults characterized by cyclic frequencies. However, as machinery can experience wear and tear under pressure and high-speed conditions, bearing degradation can result in fault features at varying cyclic frequencies. To enhance and optimize the adaptability of the ACYCBD method for such scenarios, we proposed optimal adaptive maximum second-order cyclostationary blind deconvolution (OACYCBD) to effectively filter noise from signals associated with bearing degradation. OACYCBD proved particularly well-suited for analyzing denoised signals stemming from bearing degradation across a wide range of frequencies.

The Proposed OACYCBD Method: Although ACYCBD can detect bearing faults characterized by cyclic frequencies, challenges arise when dealing with high pressures and speeds. Bearing degradation results in the accumulation of fault features at varying cyclic frequencies, necessitating adaptability enhancements for the ACYCBD method.

To advance the application of ACYCBD in bearing degradation, we introduced OACYCBD, which leverages a Monte Carlo PDF to optimize the filtering process. A probability density function (PDF) of Monte Carlo assesses condition characteristics and detects subtle dissimilarities within vibration signals, optimizing the weight coefficients of ACYCBD.

We also replaced the traditional iteration process of ACYCBD with cross-entropy, which efficiently updated the optimal filter coefficients, leading to improved filtering performance. As a result, OACYCBD excelled at filtering noise signals associated with bearing degradation, particularly when dealing with variable frequency characteristics, and outperformed standard ACYCBD when extracting features from bearing degradation.

Vibration signals refer to those obtained during the deterioration or performance loss of

the bearing. A PDF [40] is a mathematical tool to describe the probability distribution of a random variable. In the context of bearing conditions, a PDF can also be used to represent the likelihood of various levels of bearing states under different operating conditions. A PDF therefore proves invaluable in assessing condition characteristics for vibrating bearings.

Monte Carlo methods can help quantify subtle differences within the PDFs of vibration signals. Through these methods, a PDF can effectively use the following functions to demonstrate its performance [82].

$$p = \left(1 - e^{-x^2/2\delta^2}\right) \quad (4.19)$$

where x is the variable data and δ is the standard deviation. As shown in Figure 4.4, a PDF can model the density point and slight dissimilarities in a Monte Carlo simulation with a random variable. It can show that δ is critical to performance and requires an updating process in different conditions.

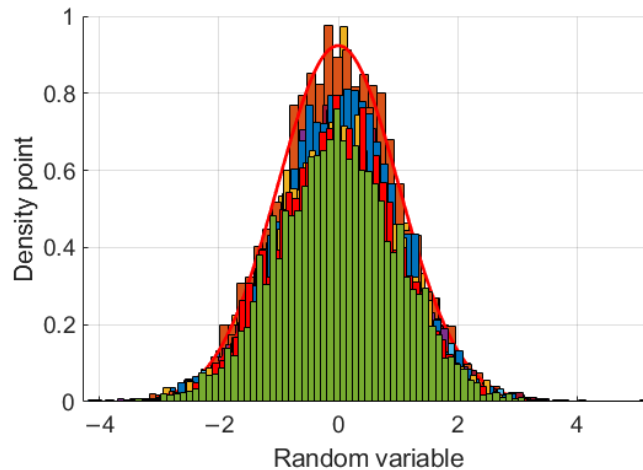


Figure 4.4. The density distribution of a Monte Carlo simulation using a random variable.

In the context of MED, CYCBD, and ACYCBD filtering methods, the convergence criteria continue to rely on traditional criteria, typically when the satisfaction of certain key values and predefined iteration numbers are involved. However, in recent years, the growing popularity of deep learning has introduced novel approaches to optimization. The use of cross-entropy has gained significant traction within the deep learning community due to its ability to effectively update parameters and yield favorable results [41], such as:

$$loss = T \ln Y + (1 - T) \ln(1 - Y) \quad (4.20)$$

where T is the targeted value and Y is the prediction value.

The OACYCBD procedure is shown in Figure 4.5 and described as follows:

Step 1: Set initial parameters for the vibration signal x , including a convergence criterion ε_0 , maximum iteration number N_{max} , filter length L , and initial filter coefficient h .

Step 2: Calculate the temporary filtering signal S from the vibration signals using initial parameters, and then apply a Monte Carlo PDF that optimizes the temporary filtering signals to make an assessment. This can assess condition characteristics and measure slight dissimilarities to estimate signals.

Step 3: Apply an EHPS to estimate the cyclic frequency of estimated signals and analyze the amplitude envelope spectrum.

Step 4: Detect the estimated cyclic frequency with the global maximum amplitude from a specified frequency range in EHPS.

Step 5: Obtain the correlation matrix R_{XX} , the weight matrix W , and the weighted correlation matrix R_{XWX} , and then update the filter coefficients in the maximum eigenvalue for the eigenvalue problem.

Step 6: Replace the traditional convergence criterion of ACYCBD with cross-entropy, return to Step 2, update the filter coefficient h to the next similar cyclic steps, and end with the convergence criterion.

Step 7: Finish with the output filtered signal.

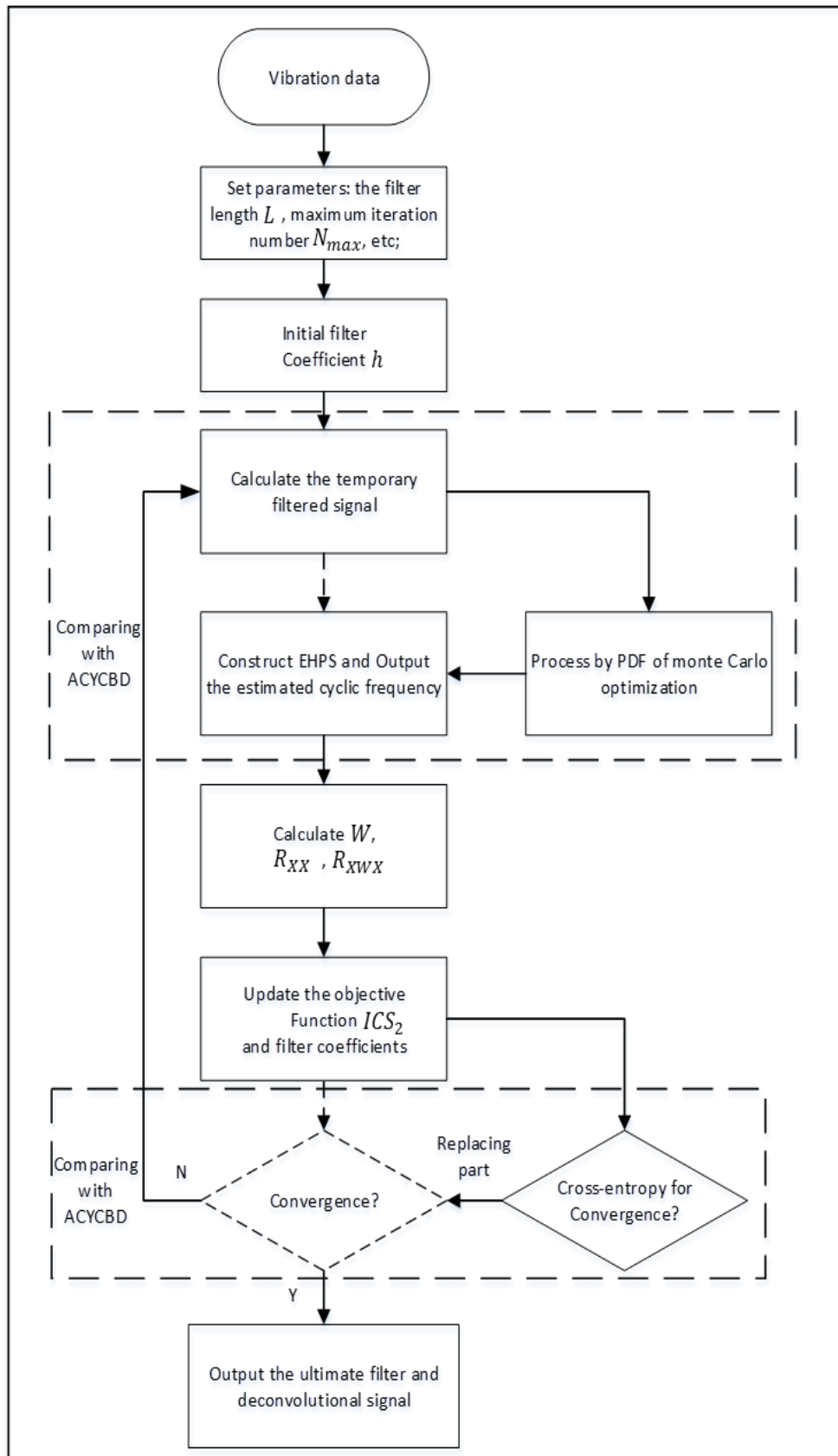


Figure 4.5. Flowchart of the proposed OACYCBD.

To demonstrate the performance of the proposed methods on filtering noise signals, vibration signals were utilized to verify the effectiveness of OACYCBD and ACYCBD (Figures 4.6–4.8). In the vibration signals, feature impulse signals were generated when the rollers reached the damage point, but because they were mixed with noise signals, the amplitude of the noise was greater than the pulse signal, and it was not easy to identify the fault information before filtering processing.

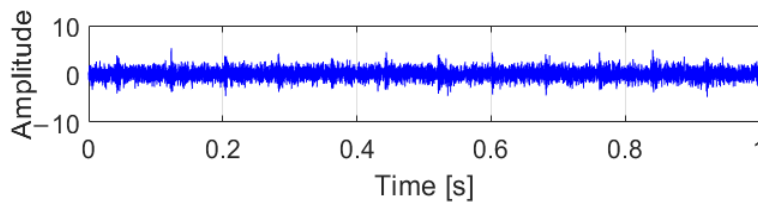
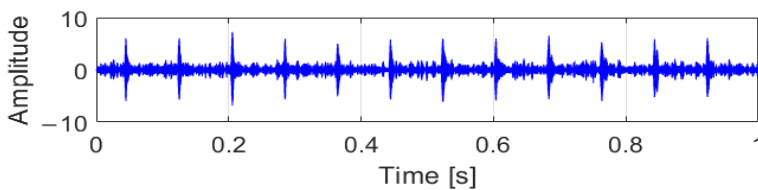
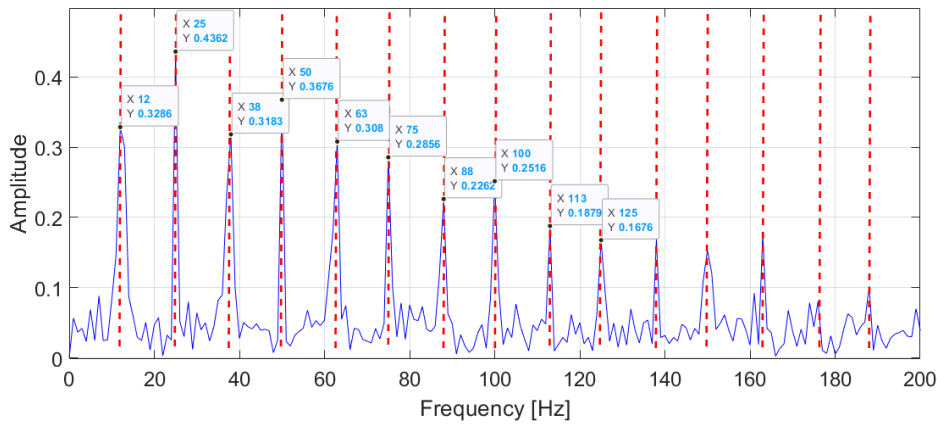


Figure 4.6. Raw vibration signals.

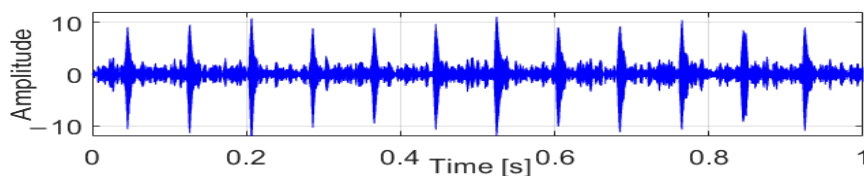


(a)



(b)

Figure 4.7. Results from ACYCBD: (a) denoised signal in the time domain; (b) envelope spectrum.



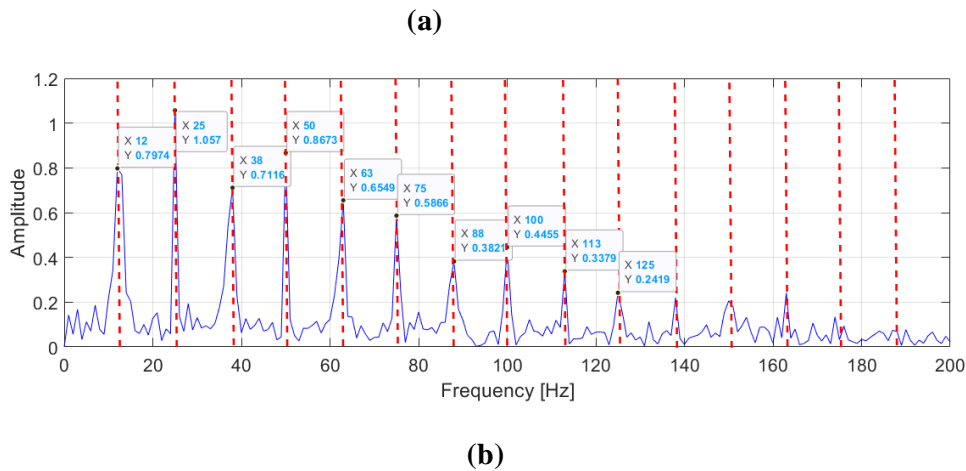


Figure 4.8. Results obtained from OACYCBD: (a) the denoised signal; (b) envelope spectrum.

The filtering results obtained using ACYCBD are depicted in Figure 4.7. To further analyze the processed signals, an envelope spectrum was used to derive the autocorrelation function, which effectively revealed energy modulation patterns. In this analysis, the fault frequency had a clear and unmistakable peak at 12 Hz. By calculating frequency multiplications within the interval [12, 25, 38, 50, 63, 75, 88, 100, 113, 125 ...] Hz, distinct peaks emerged at frequencies such as 25, 38, 50, ..., which were close to double, triple, and quadruple the fault frequency. These observed fault characteristics provided valuable insights for diagnosis and assessment.

Subsequently, the OACYCBD filtering method was used to eliminate noise, and its effectiveness was verified through envelope spectrum analysis. The results were striking, with clear and distinct spectral lines. The fault frequency at 12 Hz was readily identifiable and more pronounced compared with ACYCBD processing. The extraction of frequency multiplications, such as [12, 25, 38, 50, 63, 75, 88, 100, 113, 125 ...], was notably accurate, with peak frequencies closely aligned with 1–10 times the fault frequency.

At a peak frequency of 12 Hz, the amplitude achieved by OACYCBD was 0.79, while ACYCBD yielded an amplitude of 0.328. Similar comparisons across various frequencies consistently showed higher amplitudes with OACYCBD. These results unequivocally demonstrated that OACYBD filtering outperformed ACYCBD.

In line with the earlier descriptions, the vibration signals were primarily decomposed into feature responses. Analysis of amplitudes revealed that periodic fault impulses were successfully extracted from noisy signals using both OACYCBD and ACYCBD. However, the envelope spectrum highlights that variable cyclic frequencies are more prominently

discernible in OACYCBD. These outcomes firmly establish OACYCBD’s superior performance over ACYCBD, making it better suited for health analysis. After the noise signals from bearing degradation are effectively filtered, deep learning methods can be applied to predictions of bearing degradation. A crucial element in this process is the health index, which is a fundamental component of machinery degradation assessments. An effective health index strategy is pivotal in analyzing critical aspects of equipment degradation and quantifying various stages of health conditions.

Following the filtration of noise signals, a novel health index was introduced to assess the RUL of the machinery. This innovative method operates in the time domain, allowing it to gauge bearing degradation under varying conditions of pressure and speed and reveal the stages of health conditions in different scenarios.

In this paper, a health index was developed based on the “peaks theory”, in which peaks are identified by analyzing changes in the slope or curvature of the signal. Once these peaks are detected, further analysis can be conducted on the identified points [42]. The peak information is shown in Figure 4.9.

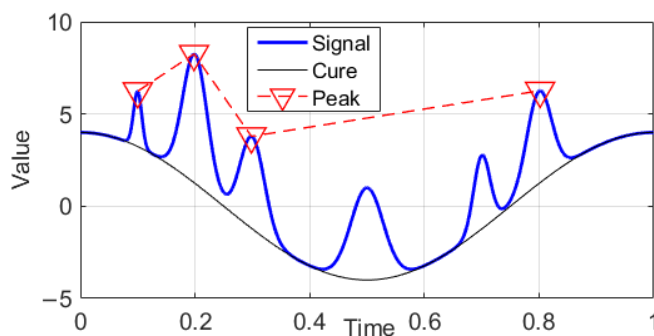


Figure 4.9. The peak signal theory.

Vibration signals (x_1, \dots, x_n) are treated as input data. First, a search for local maxima (peaks, p) from the input data is conducted, after which the average of peaks is calculated, the variance with input signals is evaluated, and the squares of the variance are summed. Finally, we divide the sum and take the square as the result, as presented in Equation (85).

$$HI = \sqrt{\frac{1}{n} \sum \left(\frac{1}{p} \sum x_p - x \right)^2} \quad (4.21)$$

4.2.3. Convolutional LSTM autoencoder

In this study, we develop a convolutional LSTM autoencoder to address the transformer problem with convolutional LSTM in forecasting. The proposed method consists of a transformer theory that can transform convolutional layers and LSTM architecture into encoded features. The model is scalable to encode features by a mixed model of convolutional layers and LSTMs [59-62].

In the architecture of the proposed method, the convolutional layer utilizes kernels to achieve convolution operation, which can filter input data to extract feature information. The formula is shown as follows:

$$y_i^{l+1}(j) = K_i^l * x^l(j) + b_i^l \quad (4.22)$$

where $x^l(j)$ represents input data, K_i^l denotes the kernel, b_i^l is bias, $*$ represents the dot product, and $y_i^{l+1}(j)$ is the computational result.

Figure 4.10 depicts the fundamental structure of the LSTM, which consists primarily of a cell, an input gate, a forget gate and an output gate. The cell controls the flow of information. A Forget gate decides which information to remove from a previous state, an input gate decides which useful information to store in the current state, and an output gate decides which information to output in the current state. The architecture makes use of disadvantages to maintain useful, long-term dependencies for prediction. All formulations are shown below.

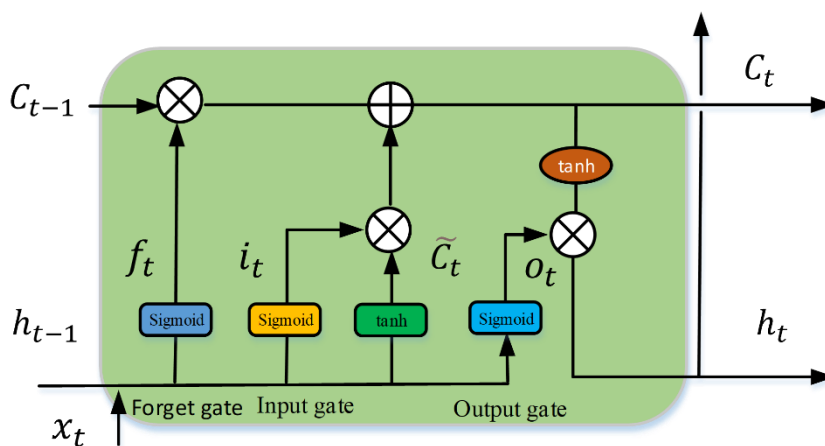


Figure 4.10. The LSTM constituted element.

$$f_t = \text{sigmoid}(W_f x_t + U_f h_{t-1} + b_f) \quad (4.23)$$

$$i_t = \text{sigmoid}(W_i x_t + U_i h_{t-1} + b_i) \quad (4.24)$$

$$o_t = \text{sigmoid}(W_o x_t + U_o h_{t-1} + b_o) \quad (4.25)$$

$$\tilde{C}_t = \tanh(W_c x_t + U_c h_{t-1} + b_c) \quad (4.26)$$

$$C_t = f_t \odot C_{t-1} + i_t \odot \tilde{C}_t \quad (4.27)$$

$$h_t = o_t \odot \tanh(C_t) \quad (4.28)$$

Where the vector x_t denotes the input data process; $W, U,$ and b are parameters; f_t represents the forget gate activation; i_t represents the input gate activation; o_t represents the output gate activation; h_t represents the hidden state vector; \tilde{C}_t presents cell input activation, and C_t represents the cell state vector.

The architecture of the convolutional LSTM autoencoder is shown in Figure 4.11.

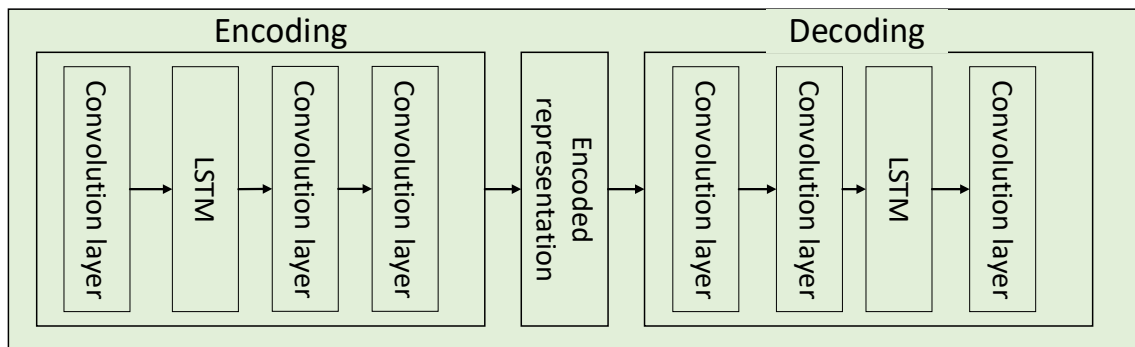


Figure 4.11. Illustration of the convolutional LSTM autoencoder.

Parameters of the convolutional layers and the LSTM of the architecture of the convolutional LSTM autoencoder are shown in Table 4.1.

Table 4.1. Parameters for the ALSTM architecture.

	Layer Type	Kernel/Stride
Encoding	Convolution	$64 \times 1/16 \times 1$
	Convolution	$64 \times 1/16 \times 1$

	LSTM	16 units
	Convolution	$64 \times 1/16 \times 1$
	Convolution	$64 \times 1/16 \times 1$
Decoding	LSTM	16 units
	Convolution	$64 \times 1/16 \times 1$
	Convolution	$64 \times 1/16 \times 1$

4.2.4. The Hybrid Invertible Neural Network

In this paper, we introduce a HINN designed to address inverse prediction problems in forecasting. Our proposed method incorporates an invertible sub-network capable of performing a one-to-one mapping from feature information to an intermediate encoded feature. The model's scalability is achieved through a combination of the encoded feature's mixture model and LSTM. Furthermore, invertible flow mapping is facilitated by leveraging theories related to optimal transport and diffusion processes.

LSTM, a specialized model derived from recurrent neural networks (RNNs), has a fundamental structure illustrated in Figure 4.10. It consists primarily of a cell and three gates: an input gate, an output gate, and a forget gate. These components work together to facilitate the flow of the model's memory and information [91, 92]. The cell within LSTM retains values over arbitrary time intervals, and the three gates play crucial roles in governing the information flow within the cell. Forget gates determine which information to discard from the previous state, input gates determine which pertinent information to incorporate into the current state, and output gates control the crucial information to be included in the current state. This architecture mitigates the limitations of RNNs and enables the retention of essential long-term dependencies for prediction. Detailed mathematical formulations are presented below.

In the basic invertible nonlinear transformation, the forward neural network $F(u) = v$, the invertible mapping $F^{-1}(v) = u$, the probability satisfies $\theta \sim p(\theta|x)$ and a Gaussian latent

variable z , and $\theta = F^{-1}(z; x)$ with $z \sim N(z|0, \mathbb{I})$ following $\theta \sim p(\theta|x)$ [100]. $N(z|0, \mathbb{I}) \propto \exp(-\frac{1}{2}z^T z)$, the basic building block of the invertible neural network, is the affine coupling layer. The approach works by splitting the input data u into an average of two parts $[u_1, u_2]$, as shown in Figure 4.12. Using transformation through s_i, t_i , the following operation can be described:

$$v_1 = u_1 \odot \exp(s_1(u_2)) + t_1(u_2) \quad (4.29)$$

$$v_2 = u_2 \odot \exp(s_2(u_1)) + t_2(u_1) \quad (4.30)$$

where \odot is element-wise multiplication, the output is $v = [v_1, v_2]$, and $F(u_1, u_2) = (v_1, v_2)$.

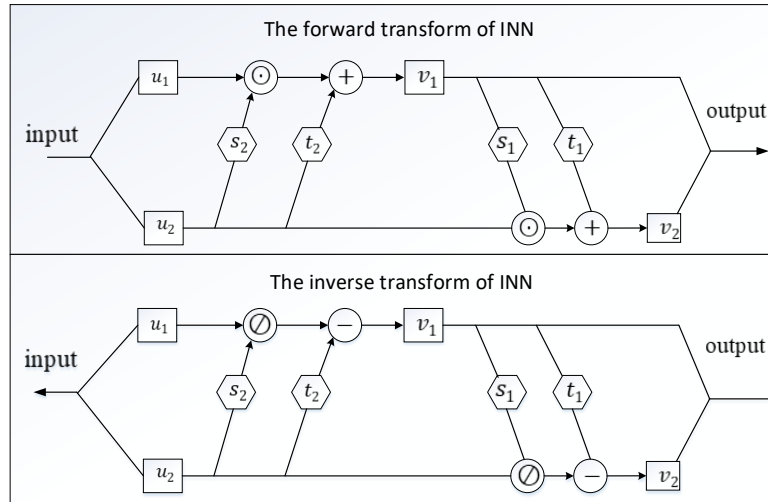


Figure 4.12. An invertible neural network.

Rearranging the previous equations, we can recover $[u_1, u_2]$ from $[v_1, v_2]$ to compute the inverse, and the invertible operation can be calculated by:

$$u_2 = (v_2 - t_1(v_1)) \odot \exp(-s_1(v_1)) \quad (4.31)$$

$$u_1 = (v_1 - t_2(u_2)) \odot \exp(-s_2(u_2)) \quad (4.32)$$

$$F^{-1}(v_1, v_2) = (u_1, u_2) \quad (4.33)$$

In the HINN architecture shown in Figure 4.13, we optimized the parameters of the LSTM neural network jointly with those of the INN chain via backpropagation. To incorporate the

input data, the proposed method can be augmented by taking h_t as an additional input and then calculating the output as

$$v_1 = u_1 \odot \exp(s_1(u_2, h_t)) + t_1(u_2, h_t) \quad (4.34)$$

$$v_2 = u_2 \odot \exp(s_2(u_1, h_t)) + t_2(u_1, h_t) \quad (4.35)$$

The entire invertible chain can be expressed as $F(\theta; h_t) = z$, together with the inverse operation $F^{-1}(z; h_t) = \theta$, $\theta \sim p(\theta|x)$. $N(z|0, \mathbb{I}) \propto \exp(-\frac{1}{2}z^T \mathbb{I} z)$.

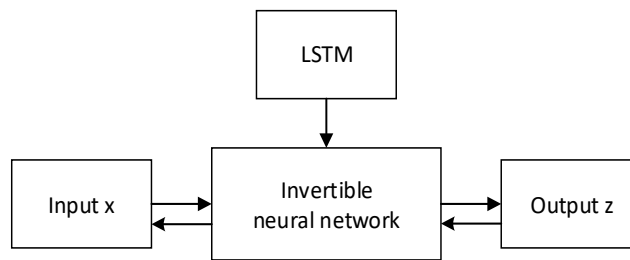


Figure 4.13. An illustration of the proposed hybrid invertible neural network.

4.3. Methodology

4.3.1. ACYCBD and Convolutional LSTM autoencoder for RUL prediction

The proposed prognosis approach is verified for bearing degradation, as discussed above. The proposed prognosis approach resolves three important issues for RUL prediction: the ACYCBD filtering method is utilized to remove noise and obtain signal, the new HI is designed to describe the bearing degradation efficiency, and the convolutional LSTM autoencoder mode is designed for prediction for RUL estimation. The whole process helps to determine the health of vibration bearings, as shown in Figure 4.14.

The proposed prognostic approach was validated using IMS run-to-failure data. As discussed above, this approach effectively addressed three critical challenges in the health assessment of bearing degradation:

1. ACYCBD filtering was used to eliminate noise signals from mixed vibration signals characterized by different cyclic frequencies, achieving superior feature extraction.

2. A novel health index was introduced to capture the evolving trend of bearing degradation efficiency.

3. An ALSTM model was used to predict future degradation trends in the health index for estimating the RUL.

This comprehensive process ensures the accurate assessment of the health condition of vibrating bearings.

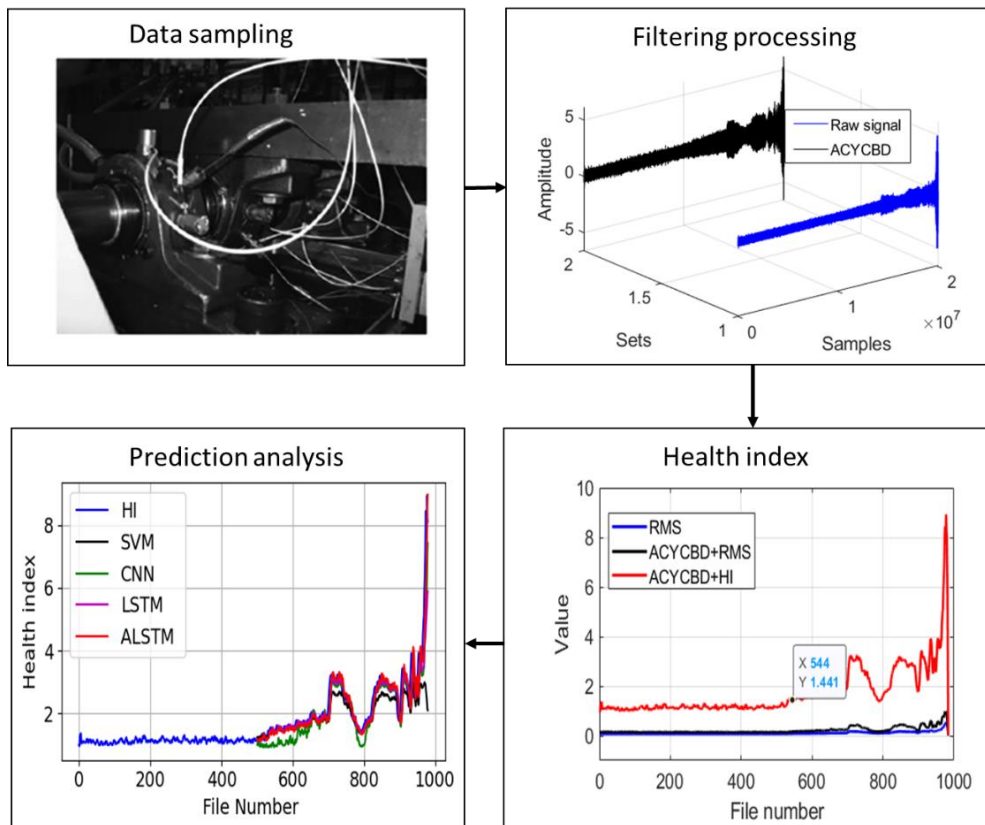


Figure 4.14. The proposed prognosis framework for whole approach processing.

4.3.2. OACYCBD and Hybrid Invertible Neural Network for RUL prediction

The proposed prognostic approach was validated using IMS run-to-failure data. As discussed above, this approach effectively addressed three critical challenges in the health assessment of bearing degradation:

1. OACYCBD filtering was used to eliminate noise signals from mixed vibration signals

characterized by different cyclic frequencies, achieving superior feature extraction.

2. A novel health index was introduced to capture the evolving trend of bearing degradation efficiency.

3. A HINN model was used to predict future degradation trends in the health index for estimating the RUL.

This comprehensive process ensures the accurate assessment of the health condition of vibrating bearings, as depicted in Figure 4.15.

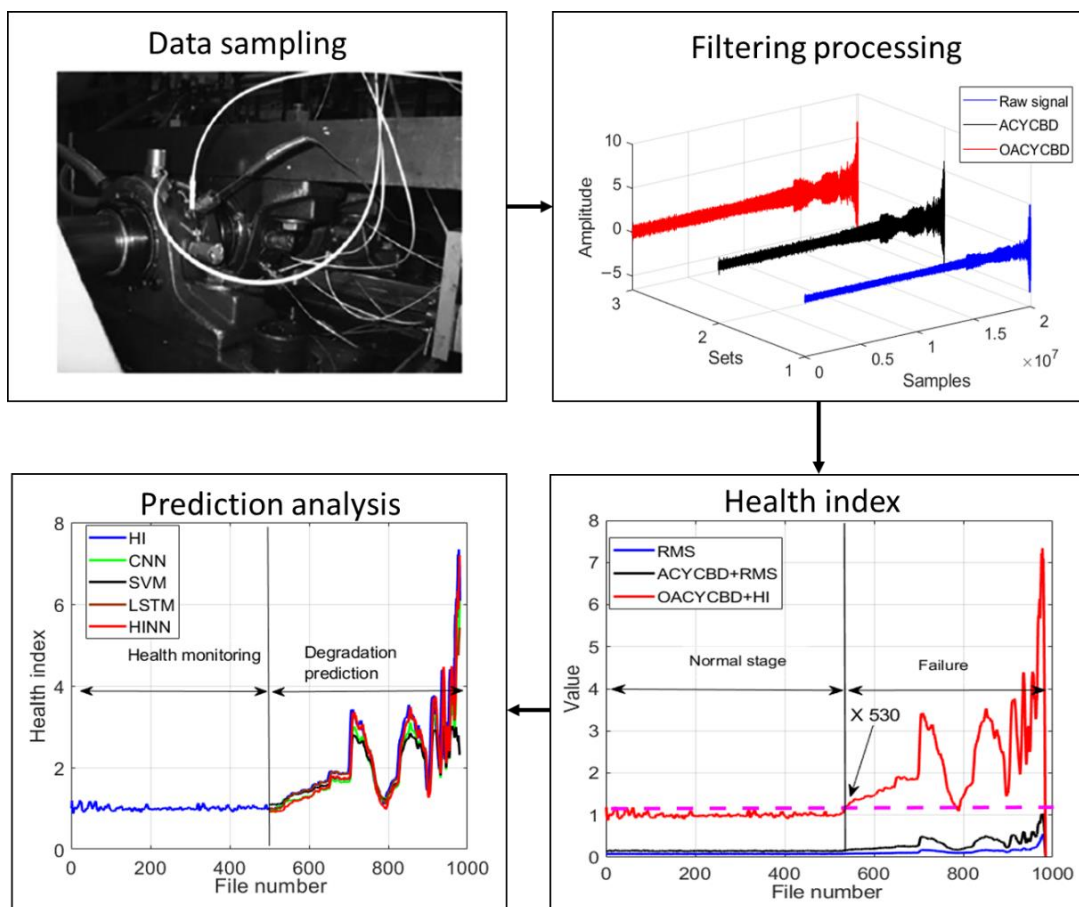


Figure 4.15. The proposed prognosis framework.

4.4. Experimental Results

4.4.1. The experiment 1

After Three data sets describe the bearing degradation experiment. Each file consists of 20,480 points for 1-second records. A total number of 984 files is saved, and the total samples are processed by filtering methods. In Figure 4.16(a), the ACYCBD method is applied to remove noise from vibration-bearing data and to extract feature signals.

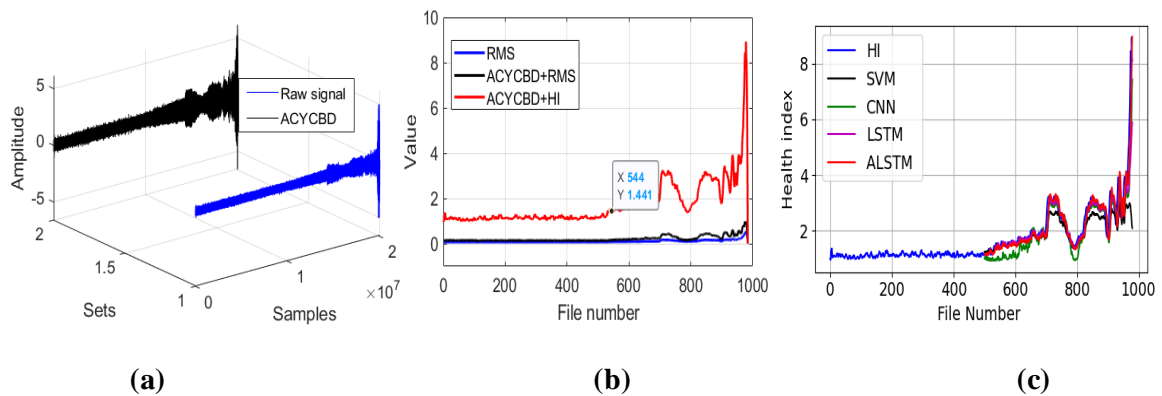


Figure 4.16. The proposed approach for the whole verified experiment: (a) raw and denoised signals, (b) RMS and HI analysis, (c) convolutional LSTM autoencoder prediction model.

After signal extraction, the HI is used to show the RUL information, in which each file with 20,480 points is calculated into a sample by the HI and RMS. As in Figure 4.16 (b), the novel HI method can measure bearing degradation to show the health conditions in different situations. The main conditions consist of normal and failure stages, where a fault onset can be observed at file number 544 by the ACYCBD and HI methods. In the ACYCBD+RMS and RMS, initial bearing degradation begins at file 730.

The convolutional LSTM autoencoder is designed to transform the nature of the network to achieve priority performance. To better show the prediction process, the total data of 980 files (removing some useless data) are used for training and testing, chosen randomly at the ratio of 1:1. The model is scalable to large memory neural networks by a mixture model of encoded features for bearing degradation as in Figure 4.16 (c). The data from 500~980 files is shown for degradation prediction. To better forecast performance compared with existing methods, the RMSE is used to evaluate the prediction performance of a convolutional LSTM Autoencoder, SVM, CNN and LSTM. The RMSE is 0.88 for SVM, 0.56 for CNN, 0.54 for LSTM, and 0.42 for ALSTM, as shown in Table 4.2. This shows that the ALSTM has better forecasting performance. Another two datasets are further used to verify the proposed

methods in Figure 4.17 and Figure 4.18.

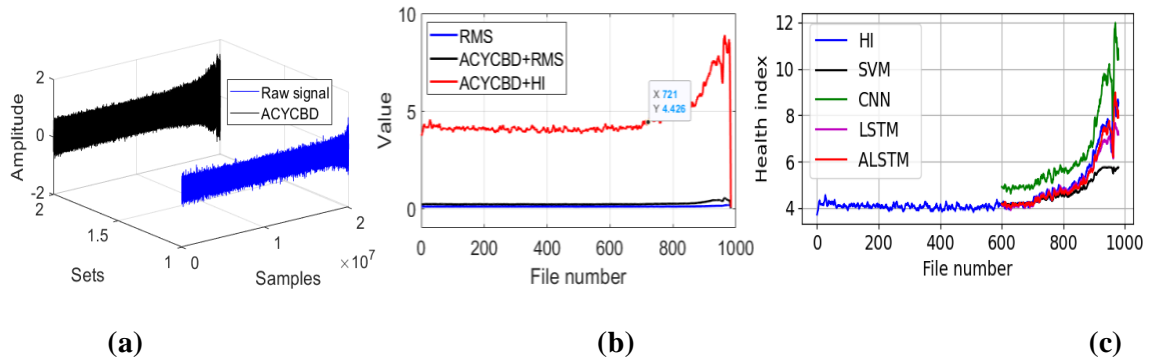


Figure 4.17. The proposed approach for the whole verified experiment: (a) raw and denoising signals, (b) RMS and health index analysis, (c) convolutional LSTM autoencoder prediction model.

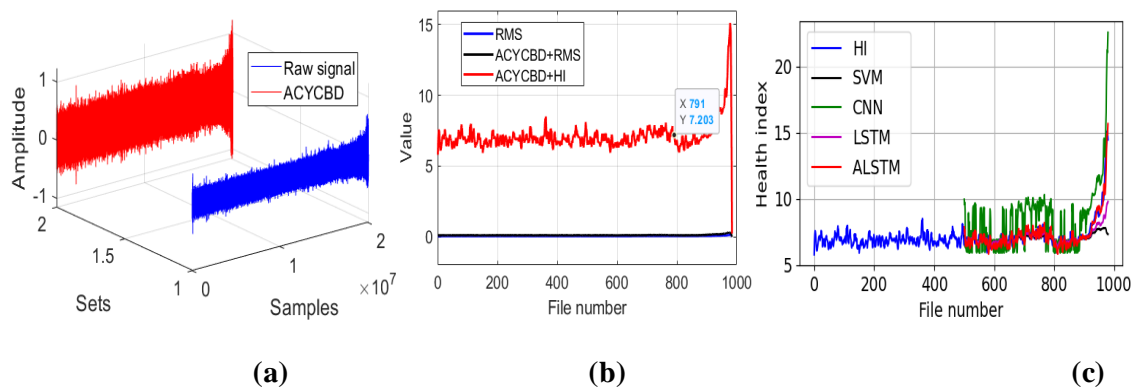


Figure 4.18. The proposed approach for the whole verified experiment: (a) raw and denoising signals, (b) RMS and health index analysis, (c) convolutional LSTM autoencoder prediction model.

Table 4.2. Method prediction comparison.

RMSE	SVM	CNN	LSTM	ALSTM
Data1	0.88	0.56	0.54	0.42
Data2	0.93	1.18	0.43	0.35
Data3	1.15	1.80	0.88	0.52

As in Figure 4.17(a), all samples are processed by ACYCBD filtering. In Figure 4.17(b), after signal extraction, the HI is used to show the RUL information, where initial bearing

degradation occurs at file 721 file by the ACYCBD and HI methods. But in the ACYCBD+RMS and RMS, bearing degradation starts at file 920. This shows that the proposed method can measure bearing degradation more efficiently. Finally, the convolutional LSTM autoencoder is used to show the prediction process. In Fig. 4.17(c), files 600~980 are shown for degradation prediction. To better forecast performance compared with existing methods, the RMSE is used to evaluate the prediction performance of the convolutional LSTM autoencoder, SVM, CNN and LSTM. The RMSE is 0.93 for SVM, 1.18 for CNN, 0.43 for LSTM, and 0.35 for ALSTM. This shows that the convolutional LSTM autoencoder has better forecasting performance.

Figure 4.18(a) shows the filtering process by ACYCBD, and the degradation measured by the HI. In Figure 4.18(b), the onset of bearing degradation can be observed at file 791 by the ACYCBD and HI methods. With the ACYCBD+RMS and RMS, bearing degradation begins after file 980. This shows that the proposed method can measure bearing degradation more efficiently. Figure 4.18(c) shows files 500~980 for degradation prediction. To better forecast performance compared with existing methods, the RMSE is used to evaluate the prediction performance of the convolutional LSTM autoencoder, SVM, CNN and LSTM. The RMSE is 1.15 for SVM, 1.80 for CNN, 0.88 for LSTM, and 0.52 for the convolutional LSTM autoencoder. This shows that the ALSTM has better forecasting performance than existing methods.

4.4.2. The experiment 2

The run-to-failure experiment can be described using three datasets, with each dataset comprising 984 vibration signal samples. Each 1 s vibration signal sample contained 20,480 data points, and all samples underwent processing using filtering methods.

Figure 4.19 a illustrates the use of a Monte Carlo PDF to optimize the filtering signal during the filtering process, which employed OACYCBD to assess the data. Additionally, cross-entropy was employed to replace the traditional iteration process found in ACYCBD. This effectively filtered noise signals originating from bearing degradation, particularly those with variable frequency characteristics.

After successfully filtering noise from bearing degradation, we proceeded to design a novel health index tailored to assess the RUL. Each sample containing 20,480 data points was

transformed into a health index using both the proposed index and RMS.

As illustrated in Figure 4.19b, the novel index method was capable of quantifying bearing degradation under various pressures and speeds in the time domain. This allowed for the visualization of distinct health condition stages in different scenarios. These conditions include the normal stage and the failure stage. An initial trend in bearing degradation became apparent as early as sample number 530, at which point both OACYCBD and the proposed health index met.

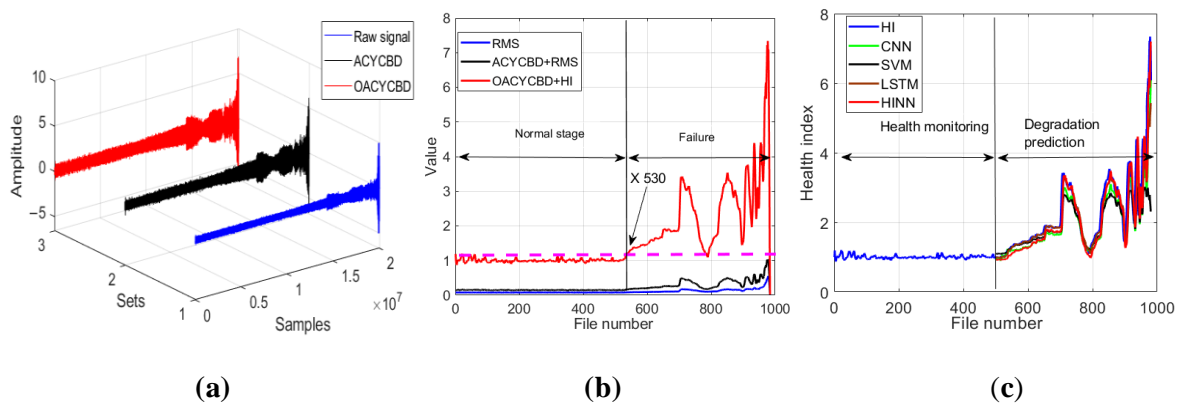


Figure 4.19. Bearing degradation processing results using different methods: (a) filtered signal by OACYCBD, (b) health index trend, and (c) forecast model using a hybrid INN model.

In contrast, when using ACYCBD+RMS and RMS alone, this initial bearing degradation trend was observed to begin with sample number 700. In addition, monotonicity was used to assess the health index construction [101]. The monotonicities were 0.11, 0.16, and 0.24 for RMS, ACYCBD+RMS, and OACYCBD+health index, respectively. The proposed method resulted in higher monotonicity compared with the reference methods. The above description shows that the proposed method is more sensitive to bearing degradation compared with either ACYCBD or RMS.

Finally, the HINN addressed the challenge of inverse prediction in memory-related tasks by framing it as a conditional memory task. To illustrate the prediction process more effectively, we used 980 samples for both training and testing chosen randomly at the ratio of 1:1. The training began with the first sample's data, which included 20,480 data points, and the testing used the data from the second sample. This process was repeated sequentially until the final sample's data were used. Each internal segment consists of one sample's data, totaling 20,480 points.

The model's ability to handle larger memory neural networks was achieved through a mixture of encoded features, particularly for bearing degradation, as depicted in Figure 4.19c. The evaluation included data from sample numbers 500 to 980 for degradation prediction. The results demonstrate superior forecasting performance when compared with SVM, CNN, and LSTM methods. The root mean square error (RMSE) evaluates the performance of different methods for forecasting [102, 103]. The RMSE was 0.799 for SVM, 0.593 for CNN, 0.53 for LSTM, and 0.485 for HINN in Table 1. This shows that HINN has superior forecasting abilities compared with SVM, CNN, and LSTM methods. We also employed two more datasets to further validate the proposed methods in the context of filtering, health index assessment, and forecasting analysis, as depicted in Figures 4.20 and 4.21. RMSE values are summarized in Figure 4.22 and Table 4.3.

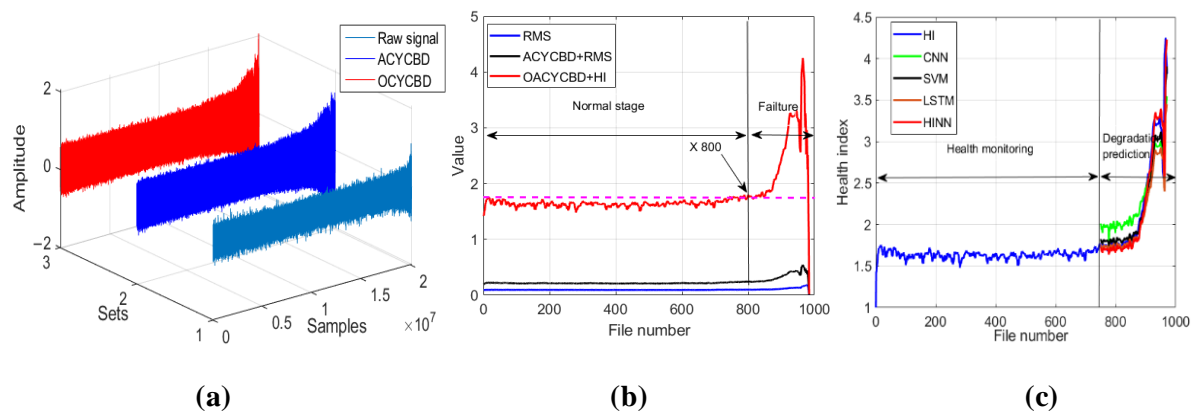


Figure 4.20. The processing for different methods on bearing degradation: (a) denoised signal by OACYCBD, (b) health index trend of bearing degradation, and (c) forecast model using a hybrid INN model.

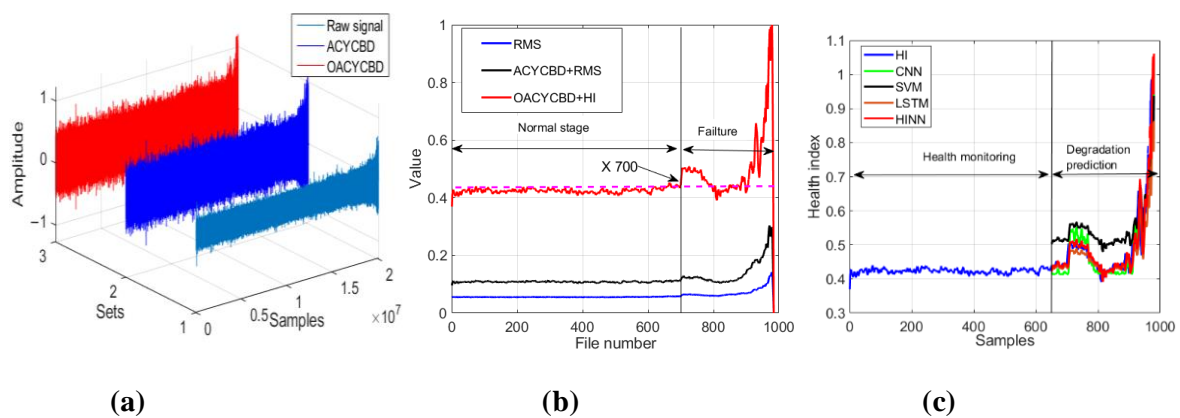


Figure 4.21. Processing for different methods for bearing degradation: (a) filtered signal by OACYCBD, (b) health index trend of bearing degradation, and (c) a forecast model on hybrid INN

model.

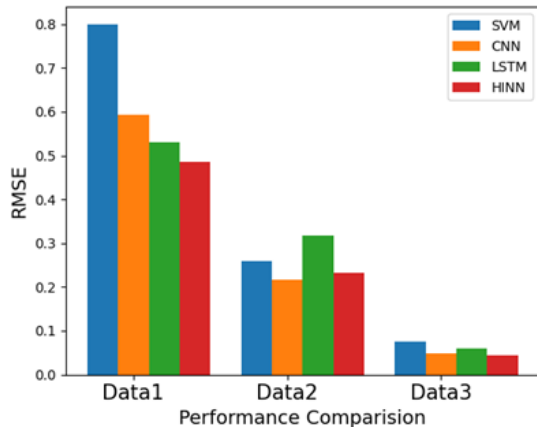


Figure 4.22. Performance comparison of model prediction.

Table 4.3. Performance comparison of model prediction.

RMSE	SVM	CNN	LSTM	HINN
Data1	0.799	0.593	0.530	0.485
Data2	0.259	0.317	0.317	0.233
Data3	0.075	0.049	0.06	0.043

In Figure 4.20a, the samples underwent processing through filtering methods. Notably, the filtering process carried out by OACYCBD and ACYCBD demonstrates its ability to effectively filter noise signals associated with bearing degradation, particularly those with a variable frequency.

In Figure 4.20b, we introduce a novel health index designed to assess the RUL. Each sample, comprising 20,480 data points, was transformed into sample-level data points using both a health index and RMS. The novel health index excels at measuring bearing degradation in the time domain, capturing distinct health condition stages in different situations, including the normal and failure stages. An initial bearing degradation trend becomes evident at sample number 800 when using OACYCBD and a health index, while ACYCBD+RMS and RMS indicate this trend began at sample number 880. This observation highlights the proposed method's enhanced sensitivity to bearing degradation when compared with ACYCBD and RMS methods.

Last, in Figure 4.20c, we address the inverse prediction problem related to memory using the HINN. By framing it as a conditional memory task, we used the complete dataset of 980 samples for both training and testing, as previously described. Results from sample numbers 750 to 980 are presented for degradation predictions. These results demonstrate superior forecasting performance compared with SVM, CNN, and LSTM methods. To quantitatively evaluate performance, we calculated the RMSE, with values of 0.259 for the SVM, 0.317 for the CNN, 0.317 for LSTM, and 0.233 for the HINN. These values highlight HINN's superior forecasting performance compared with the SVM, CNN, and LSTM methods.

In Figure 4.21a, the effectiveness of the filtering process carried out by OACYCBD and ACYCBD is evident. The optimal OACYCBD method proved its ability to filter out noise signals associated with bearing degradation, particularly those characterized by variable frequency characteristics.

Continuing with Figure 4.21b, we utilize the novel HI designed for condition assessment. Each sample, comprising 20,480 data points, is transformed into a single point using both HI and RMS. The novel HI method excels at measuring bearing degradation in the time domain, effectively capturing distinct health condition stages in different scenarios, including the normal stage and the failure stage. Notably, an initial bearing degradation trend is observable at sample number 700 when employing OACYCBD and HI, whereas ACYCBD+RMS and RMS indicate this trend starting after sample number 730. This demonstrates the proposed method's heightened sensitivity to bearing degradation compared to ACYCBD and RMS methods.

Finally, in Figure 4.21c, we delve into the inverse prediction problem employing HINN. As previously outlined, we use the complete dataset of 980 samples for both training and testing. Training commenced with data from the first sample, which comprises 20,480 data points, with testing progressing through subsequent samples sequentially. In this instance, data from sample numbers 650 to 980 are presented for degradation predictions. The outcomes unmistakably exhibit superior forecasting performance when compared to SVMs, CNNs, and LSTMs. To provide a quantitative assessment of performance, we compute the RMSE, yielding values of 0.075 for SVMs, 0.049 for CNNs, 0.060 for LSTM, and 0.043 for HINN. These RMSE values underscore HINN's superior forecasting performance in contrast to SVM, CNN, and LSTM methods.

We applied the proposed methods, namely OACYCBD+HI, ACYCBD+RMS, and RMS,

to demonstrate the comparative analysis of different degradation trends. In this section, we explore distinct approaches encompassing filtering methods and health indices to investigate bearing-condition monitoring and predict trends related to RUL of bearings undergoing gradual deterioration and performance loss over time. The results convincingly demonstrate that the proposed method exhibits heightened sensitivity to bearing degradation compared with other methods. Additionally, a HINN was employed to forecast bearing degradation, and the results underscore its superior forecasting performance when contrasted with SVM, CNN, and LSTM methods.

4.5. Conclusions

In this study, ACYCBD is used to remove noise from vibration signals, and HI is utilized to measure bearing degradation for condition investigation. Also, the convolutional LSTM autoencoder is constructed to predict RUL trends for bearing degradation. Per the above description, a new hybrid approach including a filtering method, HI, and a forecasting model improves fault diagnosis and monitoring for health conditions of rotating machinery. Compared with ACYCBD, RMS, and LSTM, the proposed method showed the greatest performance in fault recognition for rotating machinery.

ACYCBD is used to filter noise signals and identify fault features of bearing degradation with the cyclic frequency of vibrating signals. This method can avoid noise interference to identify bearing degradation, enhancing prognostic and health management under different operation conditions. ACYCBD performs well for feature extraction indicating bearing degradation.

After processing by the ACYCBD method, based on peak value properties, an HI is utilized to measure health conditions for vibration bearings. The HI can assess conditions of bearing degradation, showing greater sensitivity to RUL than existing methods.

The convolutional LSTM autoencoder can assess the RUL of bearings and show better prognostics and health management, showing greater performance than SVM, CNN, and LSTM methods.

In this paper, we introduced an OACYCBD method aimed at extracting essential features from mixed vibration signals. These signals were subsequently processed using a novel health

index, enabling the analysis of comprehensive health conditions linked to bearing degradation. Additionally, we developed a HINN to predict the health condition of bearing degradation. This holistic approach combines filtering techniques, health index analysis, and predictive modeling to significantly enhance the diagnosis and monitoring of rotating machinery health.

Our experiments have clearly demonstrated the superiority of the proposed method in comparison with ACYCBD, RMS, and LSTM. Several key findings support this conclusion. First, ACYCBD, while capable of identifying fault features with cyclic frequency in vibrating bearing signals, falls short of addressing real-world bearing degradation, which involves the accumulation of fault features at variable cyclic frequencies under conditions of high pressures and speed. OACYCBD addresses this limitation effectively by using a probability density function (PDF) of Monte Carlo to assess condition characteristics and measure subtle differences in vibration signals. Furthermore, it replaces the traditional iteration process of ACYCBD with cross-entropy, resulting in optimized filter coefficients. As a result, OACYCBD significantly outperformed ACYCBD in feature extraction for bearing degradation, providing superior noise signal filtration for variable frequency characteristics.

Second, and following noise signal filtration, we introduced a novel health index that uses peak properties and the square of the arithmetic mean to analyze critical components of equipment degradation and measure various health condition stages. This method is more sensitive to bearing degradation and health condition stages than the ACYCBD+RMS method is.

Third, in our hybrid invertible neural network, we combined INN architecture with LSTM. This model effectively assessed the damage-accumulation process associated with bearing degradation and delivered superior performance in PHM for bearing degradation. In data 1, the results demonstrate superior forecasting performance when compared with SVM, CNN, and LSTM methods. The root mean square error (RMSE) evaluates the performance of different methods for forecasting. The RMSE was 0.799 for SVM, 0.593 for CNN, 0.53 for LSTM, and 0.485 for HINN. In data 2, To quantitatively evaluate performance, we calculated the RMSE, with values of 0.259 for the SVM, 0.317 for the CNN, 0.317 for LSTM, and 0.233 for the HINN. In data 3, the outcomes unmistakably exhibit superior forecasting performance when compared to SVMs, CNNs, and LSTMs. To provide a quantitative assessment of performance, we compute the RMSE, yielding values of 0.075 for SVMs, 0.049 for CNNs, 0.060 for LSTM, and 0.043 for HINN. Notably, it outperformed SVMs, CNNs, and LSTMs

in predicting health conditions.

In summary, our research presents a comprehensive hybrid approach that excels in fault diagnosis and health monitoring for rotating machinery. The proposed methods, including advanced filtering, a novel health index analysis, and forecasting models, collectively represent a significant improvement in the recognition of faults in rotating machinery, particularly in scenarios in which bearing degradation involves variable cyclic frequencies.

In the future, multiple sensor inputs can be used to predict the RUL of the bearing. Furthermore, 2D vibration images can be utilized in the future for the prognosis of rotating machinery. Furthermore, the filtering process in the proposed method is computationally expensive. Therefore, in the future, the proposed method can be modified to reduce the computational complexity of the prognosis.

Chapter 5

Summary of Contributions and Future Work

The main contributions of this dissertation and future aspects of the current work area given in this chapter. Section 5.1 highlights the main contributions of this dissertation whereas future research direction is given in section 5.2.

5.1. Summary of Contributions

The primary objectives of this thesis are to develop effective artificial intelligence techniques for fault diagnosis of rolling element bearings, especially in feature extraction and fault recognition by using signal processing methods and artificial intelligence techniques. In this regard, the contributions have been made as follows:

In Chapter 3, to address fault classification problems of rolling element bearings, a novel hybrid deep learning method (NHDLM) based on Extended Deep Convolutional Neural Networks with Wide First-layer Kernels (EWDCNN) and long short-term memory (LSTM) is proposed for fault classification. The proposed method further improves the performance of fault classification on rolling element bearings.

In Chapter 4, the ACYCBD method is applied to remove noise signals from vibration signals, and then a novel health index (HI) is designed to analyze health conditions for the denoising signal, finally, the autoencoder can achieve transform convolutional LSTM to develop a convolutional LSTM autoencoder (ALSTM) model, ALSTM model is applied to forecast the trend for rolling element bearings, this proposed method is designed to transformer convolutional recurrent nature of the network, which can achieve high prediction accuracy on RUL estimate of rolling element bearings and better prognostics and health management for rolling element bearings.

In Chapter 4, an OACYCBD method is designed to extract essential features from mixed vibration signals. OACYCBD addresses traditional ACYCBD limitations effectively by using a probability density function (PDF) of Monte Carlo to assess condition characteristics and measure subtle differences in vibration signals. And then, these signals were subsequently processed using a novel health index, enabling the analysis of comprehensive health conditions linked to bearing degradation. The novel health index uses peak properties and the

square of the arithmetic mean to analyze critical components of equipment degradation and measure various health condition stages. Additionally, we combined INN architecture with LSTM to develop a HINN for predicting the health condition of bearing degradation. This model effectively assesses the damage-accumulation process associated with bearing degradation and delivers superior performance in PHM for bearing degradation. These above approaches combine filtering techniques, health index analysis, and predictive modeling to significantly enhance the diagnosis and monitoring of rolling element bearings.

5.2. Future work

The experiment proved that the proposed NHDLM method has better performance than the existing CNN, WDCNN, and EWDCNN methods. NHDLM can achieve greater prediction accuracy on different fault styles of vibration signals. Before deep learning methods process datasets, denoising preprocessing methods were not used. Therefore, some denoising methods can be used to preprocess and improve the performance of deep learning methods in the future.

In the future, multiple types of sensors will be applied to the RUL prediction of the bearing. Furthermore, 2D vibration images may be used in the feature analysis for the prognosis of the vibration bearings. Furthermore, the denoising step in the filtering method is computationally expensive for mixed vibration signals. As a result, in the future, the suggested approach method should be altered to lower the computing complexity for the forecast. The effectiveness of the proposed approach heavily relies on the quality of the data, and a signal processing method could help alleviate this limitation for data cleaning. The proposed approach is used for the prediction of the RUL of the degradation of real bearings. However, it demonstrates that real-world applicability could be constrained by various factors that impact the degradation of bearings, such as the pressures and speeds for the application. It is essential to evaluate the robustness of the approach across diverse real-world studies in the future.

Publications

• International Journal Papers

1. **Gao, Y.,** Kim, C. H., & Kim, J.-M. (2021). A Novel Hybrid Deep Learning Method for Fault Diagnosis of Rotating Machinery Based on Extended WDCNN and Long Short-Term Memory. *Sensors*, 21(19), 6614. <https://doi.org/10.3390/s21196614>.
2. **Gao, Y.,** Piltan, F., & Kim, J.-M. (2022). A Hybrid Leak Localization Approach Using Acoustic Emission for Industrial Pipelines. *Sensors*, 22(10), 3963. <https://doi.org/10.3390/s22103963>.
3. **Gao, Y.,** Piltan, F., & Kim, J.-M. (2022). A Novel Image-Based Diagnosis Method Using Improved DCGAN for Rotating Machinery. *Sensors*, 22(19), 7534. <https://doi.org/10.3390/s22197534>.
4. Toma, R. N., **Gao, Y.,** Piltan, F., Im, K., Shon, D., Yoon, T. H., Yoo, D.-S., & Kim, J.-M. (2022). Classification Framework of the Bearing Faults of an Induction Motor Using Wavelet Scattering Transform-Based Features. *Sensors*, 22(22), 8958. <https://doi.org/10.3390/s22228958>.
5. **Gao, Y.,** Ahmad, Z., & Kim, J.-M. (2024). Fault Diagnosis of Rotating Machinery Using an Optimal Blind Deconvolution Method and Hybrid Invertible Neural Network. *Sensors*, 24(1), 256. <https://doi.org/10.3390/s24010256>.
6. **Gao, Y.,** Ahmad, Z., & Kim, J.-M. (2024). The Prediction of the Remaining Useful Life of Rotating Machinery Based on an Adaptive Maximum Second-Order Cyclostationarity Blind Deconvolution and a Convolutional LSTM Autoencoder. *Sensors*, 24(8), 2382. <https://doi.org/10.3390/s24082382>.

• Book Chapters

1. Yangde Gao, Farzin Piltan, Zahoor Ahmad, Rafia Nishat Toma, Jong-Myon Kim, “**A Novel Fault Diagnosis Method Based on MADCNN for Rolling Bearings**”, in *Frontiers in Artificial Intelligence and Applications Ebook: Volume 360: Machine Learning and Artificial Intelligence*, page: 56 - 63, November 2022. <https://ebooks.iospress.nl/doi/10.3233/FAIA220424>
2. Rafia Nishat Toma, **Yangde Gao,** Jong-Myon Kim, “**Data-Driven Fault Classification of Induction Motor Based on Recurrence Plot and Deep Convolution Neural Network**”, in *Frontiers in Artificial Intelligence and Applications Ebook: Volume 360: Machine Learning and Artificial Intelligence*, page: 64 – 71, November 2022. <https://ebooks.iospress.nl/doi/10.3233/FAIA220425>.

- **International Conference**

1. Yangde Gao, Farzin Piltan, Zahoor Ahmad, Rafia Nishat Toma, Jong-Myon Kim, “**A Novel Fault Diagnosis Method Based on MADCNN for Rolling Bearings**”, The 4th International Conference on Machine Learning and Intelligent Systems, November 8th-11th, 2022, Seoul, South Korea.

References

- [1] Xy Wu, Y Zhang, Cm Cheng, et al. A hybrid classification autoencoder for semi-supervised fault diagnosis in rotating machinery. *Mechanical Systems and Signal Processing*, 2021, 149: 107327
- [2] W Zhang, Ch Li, Gl Peng, et al. A deep convolutional neural network with new training methods for bearing fault diagnosis under noisy environment and different working load. *Mechanical Systems & Signal Processing*, 2017, 100(FEB.1): 439-453.
- [3] C Li, Sh Zhang, Y Qin, et al. A systematic review of deep transfer learning for machinery fault diagnosis. *Neurocomputing*, 2020, 407.
- [4] P Zmarzy. Multi-Dimensional Mathematical Wear Models of Vibration Generated by Rolling Ball Bearings Made of AISI 52100 Bearing Steel. *Materials*, 2020, 13(23):5440.
- [5] R Zhao, Rq Yan a, Zh Chen, et al. Deep learning and its applications to machine health monitoring. *Mechanical Systems and Signal Processing*, 2019, 115: 213-237.
- [6] Z Ye, Jb Yu. Deep morphological convolutional network for feature learning of vibration signals and its applications to gearbox fault diagnosis. *Mechanical Systems and Signal Processing*, 161.
- [7] Lu, Q., & Li, M. (2023). Digital Twin-Driven Remaining Useful Life Prediction for Rolling Element Bearing. *Machines*, 11(7), 678. <https://doi.org/10.3390/machines11070678>.
- [8] Sanakkayala, D. C., Varadarajan, V., Kumar, N., Karan, Soni, G., Kamat, P., Kumar, S., Patil, S., & Kotecha, K. (2022). Explainable AI for Bearing Fault Prognosis Using Deep Learning Techniques. *Micromachines*, 13(9), 1471. <https://doi.org/10.3390/mi13091471>.
- [9] Zhao, X., Qin, Y., He, C., & Jia, L. (2020). Intelligent Fault Identification for Rolling Element Bearings in Impulsive Noise Environments Based on Cyclic Correntropy Spectra and LSSVM. *IEEE Access*, 8, 40925-40938. <https://doi.org/10.1109/ACCESS.2020.2976868>.
- [10] Zy Chen, A Mauricio, Wh Li, et al. A Deep Learning method for bearing fault diagnosis based on Cyclic Spectral Coherence and Convolutional Neural Networks. *Mechanical Systems and Signal Processing*, 2020, 140.
- [11] X Wang, Dx Mao, Xd Li. Bearing fault diagnosis based on vibro-acoustic data fusion and 1D-CNN network. *Measurement*, 2021, 173(6): 108518.
- [12] W Zhang, Gl Peng, Ch Li. A New Deep Learning Model for Fault Diagnosis with Good Anti-Noise and Domain Adaptation Ability on Raw Vibration Signals. *Sensors*, 2017, 17(3): 425.
- [13] Zy He, Hd Shao, X Zhong, et al. Ensemble transfer CNNs driven by multi-channel signals for fault diagnosis of rotating machinery cross working conditions - ScienceDirect. *Knowledge-Based Systems*, 207.
- [14] S Plakias, Y S. Boutalis. Fault detection and identification of rolling element bearings with Attentive Dense CNN. *Neurocomputing*, 2020, 405.
- [15] Wang, J., Wang, J., Du, W., Zhang, J., Wang, Z., Wang, G., & Li, T. (2019). Application of a New Enhanced Deconvolution Method in Gearbox Fault Diagnosis. *Applied Sciences*, 9(24), 5313. <https://doi.org/10.3390/app9245313>.
- [16] Tian, T., Tang, G.-J., Tian, Y.-C., & Wang, X.-L. (2023). Blind Deconvolution Based on Correlation Spectral Negentropy for Bearing Fault. *Entropy*, 25(3), 543. <https://doi.org/10.3390/e25030543>.

-
- [17] Gao, Y., Ahmad, Z., & Kim, J.-M. (2024). Fault Diagnosis of Rotating Machinery Using an Optimal Blind Deconvolution Method and Hybrid Invertible Neural Network. *Sensors*, 24(1), 256. <https://doi.org/10.3390/s24010256>.
- [18] Wang, Z., Zhou, J., Du, W., Lei, Y., & Wang, J. (2022). Bearing fault diagnosis method based on adaptive maximum cyclostationarity blind deconvolution. *Mechanical Systems and Signal Processing*, 162, 108018. <https://doi.org/10.1016/j.ymssp.2021.108018>.
- [19] Zhang, B., Miao, Y., Lin, J., & Yi, Y. (2021). Adaptive maximum second-order cyclostationarity blind deconvolution and its application for locomotive bearing fault diagnosis. *Mechanical Systems and Signal Processing*, 158, 107736. <https://doi.org/10.1016/j.ymssp.2021.107736>.
- [20] Gao, K.; Cai, Z.; Li, Z.; Zeng, A.; Jiang, D.; Xu, J. Comparison of data Preprocessing Methods for Support Vector Regression based Remaining Useful Life Prediction. In *Proceedings of the 2022 5th International Conference on Data Science and Information Technology (DSIT)*, Shanghai, China, 22–24 July 2022; pp. 1–5.
- [21] Islam, M.M.; Prosvirin, A.E.; Kim, J.M. Data-driven prognostic scheme for rolling-element bearings using a new health index and variants of least-square support vector machines. *Mech. Syst. Signal Process.* 2021, 160, 107853.
- [22] Wang, Y.; Zhao, Y.; Addepalli, S. Remaining Useful Life Prediction using Deep Learning Approaches: A Review. In *Proceedings of the 8th International Conference on Through-Life Engineering Service—TESConf 2019*, Cleveland, OH, USA, 27–29 October 2019.
- [23] Zhu, J.; Chen, N.; Peng, W. Estimation of Bearing Remaining Useful Life Based on Multiscale Convolutional Neural Network. *IEEE Trans. Ind. Electron.* 2019, 66, 3208–3216.
- [24] Shi, P.; Yu, Y.; Gao, H.; Hua, C. A novel multi-source sensing data fusion-driven method for detecting rolling mill health states under imbalanced and limited datasets. *Mech. Syst. Signal Process.* 2022, 171, 108903.
- [25] Ding, X.; Wang, H.; Cao, Z.; Liu, X.; Liu, Y.; Huang, Z. An Edge Intelligent Method for Bearing Fault Diagnosis Based on a Parameter Transplantation Convolutional Neural Network. *Electronics* 2023, 12, 1816.
- [26] Chen, Z.; Tu, X.; Hu, Y.; Li, F. Real-Time Bearing Remaining Useful Life Estimation based on the Frozen Convolutional and Activated Memory Neural Network. *IEEE Access* 2019, 7, 96583–96593.
- [27] Jy Wang, Jg Miao, JI Wang, et al. Fault Diagnosis of Electrohydraulic Actuator Based on Multiple Source Signals: An Experimental Investigation. *Neurocomputing*, 2020, 417(17).
- [28] H Han, H Wang, ZI Liu, et al. Intelligent vibration signal denoising method based on non- local fully convolutional neural network for rolling bearings - ScienceDirect. *ISA Transactions*, 2021.
- [29] Zy Chen, K Gryllias, Wh Li. Mechanical fault diagnosis using Convolutional Neural Networks and Extreme Learning Machine. *Mechanical Systems and Signal Processing*, 2019, 133.
- [30] S Xiang, Y Qin, Cc Zhu, et al. Long short-term memory neural network with weight amplification and its application into gear remaining useful life prediction. *Engineering Applications of Artificial Intelligence*, 2020, 91:103587-.

-
- [31] Jh Lei, C Liu, Dx Jiang. Fault diagnosis of wind turbine based on Long Short-term memory networks. *Renewable Energy*, 2019, 133(APR.): 422-432.
- [32] J Yang, G Xie, Yx Yang, et al. Deep model integrated with data correlation analysis for multiple intermittent faults diagnosis. *ISA Transactions*, 2019, 95.
- [33] Sj Hao, F-X Ge, Ym Li, et al. Multisensor Bearing Fault Diagnosis Based on One-dimensional Convolutional Long Short-Term Memory Networks. *Measurement*, 2020, 159: 107802.
- [34] Jc Shi, Dk Peng, Zx Peng, et al. Planetary gearbox fault diagnosis using bidirectional-convolutional LSTM networks. *Mechanical Systems and Signal Processing*, 162.
- [35] D ZHOU, X ZHUANG, Hf ZUO. A hybrid deep neural network based on multi-time window convolutional bidirectional LSTM for civil aircraft APU hazard identification. *Chinese Journal of Aeronautics*, 2021.
- [36] Bx Gao, Xq Huang, Js Shi, et al. Hourly forecasting of solar irradiance based on CEEMDAN and multi-strategy CNN-LSTM neural networks. *Renewable Energy*, 2020, 162.
- [37] Rathore, M. S., & Harsha, S. P. (2024). Unsupervised Domain Deep Transfer Learning Approach for Rolling Bearing Remaining Useful Life Estimation. *Journal of Computing and Information Science in Engineering*, 24(2). <https://doi.org/10.1115/1.4062731>.
- [38] Ding, A., Qin, Y., Wang, B., Cheng, X., & Jia, L. (2024). An Elastic Expandable Fault Diagnosis Method of Three-Phase Motors Using Continual Learning for Class-Added Sample Accumulations. *IEEE Transactions on Industrial Electronics*, 1–10. <https://doi.org/10.1109/TIE.2023.3301546>.
- [39] Yang, J., & Wang, X. (2024). Meta-learning with deep flow kernel network for few shot cross-domain remaining useful life prediction. *Reliability Engineering & System Safety*, 244, 109928. <https://doi.org/10.1016/j.ress.2024.109928>.
- [40] Available online: <https://uk.mathworks.com/help/predmaint/ug/similarity-based-remaining-useful-life-estimation.html> (accessed on 1 December 2022).
- [41] Available online: <https://uk.mathworks.com/help/deeplearning/ref/dlarray.crossentropy.html> (accessed on 1 December 2022).
- [42] Available online: <https://uk.mathworks.com/help/matlab/ref/peaks.html> (accessed on 1 December 2022).
- [43] Guo, X. A Novel Denoising Approach Based on Improved Invertible Neural Networks for Real-Time Conveyor Belt Monitoring. *IEEE Sens. J.* 2023, 23, 3194–3203.
- [44] Xu, C.; Cheng, X.; Xie, Y. Invertible Neural Networks for Graph Prediction. *IEEE J. Sel. Areas Inf. Theory* 2022, 3, 454–467.
- [45] Huang, J.J.; Dragotti, P.L. WINNet: Wavelet-inspired Invertible Network for Image Denoising. *IEEE Trans. Image Process.* 2022, 31, 4377–4392.
- [46] Zy He, Hd Sha, Js Cheng, et al. Support tensor machine with dynamic penalty factors and its application to the fault diagnosis of rotating machinery with unbalanced data. *Mechanical systems and signal processing*, 2020, 141(Jul.):106441.1-106441.22.
- [47] Cj Qin, G Shi, Jf Tao, et al. Precise cutterhead torque prediction for shield tunneling machines using a novel hybrid deep neural network. *Mechanical Systems and Signal Processing*, 2021, 151(6): 107386.
- [48] Feng, Y., Huang, X., Chen, J., Wang, H., & Hong, R. (2014). Reliability-based

-
- residual life prediction of large-size low-speed slewing bearings. *Mechanism and Machine Theory*, 81, 94–106. <https://doi.org/10.1016/j.mechmachtheory.2014.06.013>.
- [49] Yin, J., & Cen, G. (2022). Intelligent Motor Bearing Fault Diagnosis Using Channel Attention-Based CNN. *World Electric Vehicle Journal*, 13(11), 208. <https://doi.org/10.3390/wevj13110208>.
- [50] Song, L., Wu, J., Wang, L., Chen, G., Shi, Y., & Liu, Z. (2023). Remaining Useful Life Prediction of Rolling Bearings Based on Multi-Scale Attention Residual Network. *Entropy*, 25(5), 798. <https://doi.org/10.3390/e25050798>.
- [51] Wang, X., Hua, T., Xu, S., & Zhao, X. (2023). A Novel Rolling Bearing Fault Diagnosis Method Based on BLS and CNN with Attention Mechanism. *Machines*, 11(2), 279. <https://doi.org/10.3390/machines11020279>.
- [52] Shao, X., & Kim, C.-S. (2022). Unsupervised Domain Adaptive 1D-CNN for Fault Diagnosis of Bearing. *Sensors*, 22(11), 4156. <https://doi.org/10.3390/s22114156>.
- [53] Deng, F., Bi, Y., Liu, Y., & Yang, S. (2021). Deep-Learning-Based Remaining Useful Life Prediction Based on a Multi-Scale Dilated Convolution Network. *Mathematics*, 9(23), 3035. <https://doi.org/10.3390/math9233035>.
- [54] Yang, J., Peng, Y., Xie, J., & Wang, P. (2022). Remaining Useful Life Prediction Method for Bearings Based on LSTM with Uncertainty Quantification. *Sensors*, 22(12), 4549. <https://doi.org/10.3390/s22124549>.
- [55] Li, W., Zhang, L.-C., Wu, C.-H., Wang, Y., Cui, Z.-X., & Niu, C. (2024). A data-driven approach to RUL prediction of tools. *Advances in Manufacturing*, 12(1), 6–18. <https://doi.org/10.1007/s40436-023-00464-y>.
- [56] Qiao, M., Yan, S., Tang, X., & Xu, C. (2020). Deep Convolutional and LSTM Recurrent Neural Networks for Rolling Bearing Fault Diagnosis Under Strong Noises and Variable Loads. *IEEE Access*, 8, 66257–66269. <https://doi.org/10.1109/ACCESS.2020.2985617>.
- [57] Zhao, C., Huang, X., Li, Y., & Yousaf Iqbal, M. (2020). A Double-Channel Hybrid Deep Neural Network Based on CNN and BiLSTM for Remaining Useful Life Prediction. *Sensors*, 20(24), 7109. <https://doi.org/10.3390/s20247109>.
- [58] Zhang, F., Zhu, Y., Zhang, C., Yu, P., & Li, Q. (2023). Abnormality Detection Method for Wind Turbine Bearings Based on CNN-LSTM. *Energies*, 16(7), 3291. <https://doi.org/10.3390/en16073291>.
- [59] Zhong, Z., Zhao, Y., Yang, A., Zhang, H., & Zhang, Z. (2022). Prediction of Remaining Service Life of Rolling Bearings Based on Convolutional and Bidirectional Long- and Short-Term Memory Neural Networks. *Lubricants*, 10(8), 170. <https://doi.org/10.3390/lubricants10080170>.
- [60] Kaji, M., Parvizian, J., & van de Venn, H. W. (2020). Constructing a Reliable Health Indicator for Bearings Using Convolutional Autoencoder and Continuous Wavelet Transform. *Applied Sciences*, 10(24), 8948. <https://doi.org/10.3390/app10248948>.
- [61] Wang, C., Jiang, W., Yang, X., & Zhang, S. (2021). RUL Prediction of Rolling Bearings Based on a DCAE and CNN. *Applied Sciences*, 11(23), 11516. <https://doi.org/10.3390/app112311516>.
- [62] Ates, C., Höfchen, T., Witt, M., Koch, R., & Bauer, H.-J. (2023). Vibration-Based Wear Condition Estimation of Journal Bearings Using Convolutional Autoencoders.

-
- Sensors, 23(22), 9212. <https://doi.org/10.3390/s23229212>.
- [63] Ye, Z., Zhang, Q., Shao, S., Niu, T., & Zhao, Y. (2022). Rolling Bearing Health Indicator Extraction and RUL Prediction Based on Multi-Scale Convolutional Autoencoder. *Applied Sciences*, 12(11), 5747. <https://doi.org/10.3390/app12115747>.
- [64] Zheng Wang, etc. (2023). A Bearing Fault Diagnosis Method Based on a ResidualNetwork and a Gated Recurrent Unit under Time-Varying Working Conditions. *Sensors*, 23. <https://doi.org/10.3390/s23156730>.
- [65] L. Li, Z. Zhao, X. Zhao, et al. Gated recurrent unit networks for remaining useful life prediction. *IFAC-PapersOnLine*, 53 (2) (2020), pp. 10498-10504.
- [66] Bertocco, M.; Fort, A.; Landi, E.; Mugnaini, M.; Parri, L.; Peruzzi, G.; Pozzebon, A. Roller Bearing Failures Classification with Low Computational Cost Embedded Machine Learning. In *Proceedings of the 2022 IEEE International Workshop on Metrology for Automotive (MetroAutomotive)*, Modena, Italy, 4–6 July 2022; pp. 12–17.
- [67] Du, J.; Li, X.; Gao, Y.; Gao, L. Integrated Gradient-Based Continuous Wavelet Transform for Bearing Fault Diagnosis. *Sensors* 2022, 22, 8760.
- [68] Lei, Y.; Yang, B.; Jiang, X.; Jia, F.; Li, N.; Nandi, A.K. Applications of machine learning to machine fault diagnosis: A review and roadmap. *Mech. Syst. Signal Process.* 2020, 138, 106587.
- [69] Ding, A.; Qin, Y.; Wang, B.; Cheng, X.; Jia, L. An Elastic Expandable Fault Diagnosis Method of Three-Phase Motors Using Continual Learning for Class-Added Sample Accumulations. In *IEEE Transactions on Industrial Electronics*; IEEE: New York, NY, USA, 2023; pp. 1–10.
- [70] JDMD Editorial Office; Gebraeel, N.; Lei, Y.; Li, N.; Si, X.; Zio, E. Prognostics and Remaining Useful Life Prediction of Machinery: Advances, Opportunities and Challenges. *J. Dyn. Monit. Diagn.* 2023, 2, 1–12.
- [71] Das, O.; Bagci Das, D.; Birant, D. Machine learning for fault analysis in rotating machinery: A comprehensive review. *Heliyon* 2023, 9, e17584.
- [72] Buzzoni, M.; D’Elia, G.; Cocconcelli, M. A tool for validating and benchmarking signal processing techniques applied to machine diagnosis. *Mech. Syst. Signal Process.* 2020, 139, 106618.
- [73] Soave, E.; D’Elia, G.; Cocconcelli, M.; Battarra, M. Blind deconvolution criterion based on Fourier–Bessel series expansion for rolling element bearing diagnostics. *Mech. Syst. Signal Process.* 2022, 169, 169.
- [74] He, Z.; Chen, G.; Hao, T.; Liu, X.; Teng, C. An optimal filter length selection method for MED based on autocorrelation energy and genetic algorithms. *ISA Trans.* 2021, 109, 109.
- [75] Miao, Y.; Zhang, B.; Lin, J.; Zhao, M.; Liu, H.; Liu, Z.; Li, H. A review on the application of blind deconvolution in machinery fault diagnosis. *Mech. Syst. Signal Process.* 2022, 163, 108202.
- [76] Lopez, C.; Wang, D.; Naranjo, A.; Moore, K.J. Box-cox-sparse-measures-based blind filtering: Understanding the difference between the maximum kurtosis deconvolution and the minimum entropy deconvolution. *Mech. Syst. Signal Process.* 2022, 165, 108376.

-
- [77] Miao, Y.; Li, C.; Shi, H.; Han, T. Deep network-based maximum correlated kurtosis deconvolution: A novel deep deconvolution for bearing fault diagnosis. *Mech. Syst. Signal Process.* 2023, 189, 110110.
- [78] Buzzoni, M.; Antoni, J.; Elia, G. Blind deconvolution based on cyclostationarity maximization and its application to fault identification. *J. Sound Vib.* 2018, 432, 569–601.
- [79] Zhang, Z.; Wang, J.; Li, S.; Han, B.; Jiang, X. Fast nonlinear blind deconvolution for rotating machinery fault diagnosis. *Mech. Syst. Signal Process.* 2023, 187, 109918.
- [80] Zhang, B.; Miao, Y.; Lin, J.; Yi, Y. Adaptive maximum second-order cyclostationarity blind deconvolution and its application for locomotive bearing fault diagnosis—ScienceDirect. *Mech. Syst. Signal Process.* 2021, 158, 107736.
- [81] Gao, Y., Ahmad, Z., & Kim, J.-M. (2024). The Prediction of the Remaining Useful Life of Rotating Machinery Based on an Adaptive Maximum Second-Order Cyclostationarity Blind Deconvolution and a Convolutional LSTM Autoencoder. *Sensors*, 24(8), 2382. <https://doi.org/10.3390/s24082382>.
- [82] Miao, Y.; Zhao, M.; Lin, J.; Xu, X. Sparse maximum harmonics-to-noise-ratio deconvolution for weak fault signature detection in bearings. *Meas. Sci. Technol.* 2016, 27, 105004.
- [83] Li, X.; Wang, Y.; Tang, B.; Qin, Y.; Zhang, G. Canonical correlation analysis of dimension reduced degradation feature space for machinery condition monitoring. *Mech. Syst. Signal Process.* 2023, 182, 109603.
- [84] Liu, X.; Lei, Y.; Li, N.; Si, X.; Li, X. RUL prediction of machinery using convolutional-vector fusion network through multi-feature dynamic weighting. *Mech. Syst. Signal Process.* 2023, 185, 109788.
- [85] Wang, D.; Chen, Y.; Shen, C.; Zhong, J.; Peng, Z.; Li, C. Fully interpretable neural network for locating resonance frequency bands for machine condition monitoring. *Mech. Syst. Signal Process.* 2022, 168, 108673.
- [86] Cao, Y.; Jia, M.; Ding, Y.; Zhao, X.; Ding, P.; Gu, L. Complex domain extension network with multi-channels information fusion for remaining useful life prediction of rotating machinery. *Mech. Syst. Signal Process.* 2023, 192, 110190.
- [87] Baptista, M.L.; Henriques, E.M.; Prendergast, H. Classification prognostics approach in aviation. *Measurement* 2021, 182, 109756.
- [88] He, R.; Tian, Z.; Zuo, M. A transferable neural network method for remaining useful life prediction. *Mech. Syst. Signal Process.* 2023, 183, 109608.
- [89] Zhang, Y.; Feng, K.; Ji, J.C.; Yu, K.; Ren, Z.; Liu, Z. Dynamic Model-Assisted Bearing Remaining Useful Life Prediction Using the Cross-Domain Transformer Network. *IEEE/ASME Trans. Mechatron.* 2023, 28, 1070–1080.
- [90] Li, F.; Cheng, Y.; Tang, B.; Zhou, X.; Tian, D. Multi-layer gated temporal convolution network for residual useful life prediction of rotating machinery. *Mech. Syst. Signal Process.* 2021, 155, 107600.
- [91] Ma, M.; Mao, Z. Deep-Convolution-Based LSTM Network for Remaining Useful Life Prediction. *IEEE Trans. Ind. Inform.* 2021, 17, 1658–1667.
- [92] Zhu, Y. Hybrid scheme through read-first-LSTM encoder-decoder and broad learning system for bearings degradation monitoring and remaining useful life estimation. *Adv.*

-
- Eng. Inform. 2023, 56, 102014.
- [93] Lu, B.L.; Liu, Z.H.; Wei, H.L.; Chen, L.; Zhang, H.; Li, X.H. A Deep Adversarial Learning Prognostics Model for Remaining Useful Life Prediction of Rolling Bearing. *IEEE Trans. Artif. Intell.* 2021, 2, 329–340.
- [94] Zhao, X.; Zhang, L.; Cao, Y.; Jin, K.; Hou, Y. Anomaly Detection Approach in Industrial Control Systems Based on Measurement Data. *Information* 2022, 13, 450.
- [95] Alfarizi, M.G.; Tajiani, B.; Vatn, J.; Yin, S. Optimized Random Forest Model for Remaining Useful Life Prediction of Experimental Bearings. *IEEE Trans. Ind. Inform.* 2023, 19, 7771–7779.
- [96] Stefan, T. Radev, BayesFlow: Learning Complex Stochastic Models With Invertible Neural Networks. *IEEE Trans. Neural Netw. Learn. Syst.* 2022, 33, 1452–1466.
- [97] Yi, Q.; Zhao, C.; Wang, P. Characteristics of defect states in periodic railway track structure. *J. Low Freq. Noise Vib. Act. Control.* 2022, 41, 196–208.
- [98] Trzaska, M.; Trzaska, Z. The time domain analysis of interactions in the wheel-rail contacts due to discontinuous time periodic loads. *J. KONES* 2012, 19, 531–542.
- [99] Song, Y.; Mei, G.; Liu, Z.; Gao, S. Assessment of railway pantograph-catenary interaction performance with realistic pantograph strip imperfection. In *Vehicle System Dynamics*; Taylor & Francis: Abingdon, UK, 2023.
- [100] Available online: <https://hci.iwr.uni-heidelberg.de/vislearn/inverse-problems-invertible-neural-networks> (accessed on 1 December 2022).
- [101] Nguyen, T.K.; Ahmad, Z.; Kim, J.M. A Deep-Learning-Based Health Indicator Constructor Using Kullback–Leibler Divergence for Predicting the Remaining Useful Life of Concrete Structures. *Sensors* 2022, 5, 3687.
- [102] Yan, X.; Xia, X.; Wang, L.; Zhang, Z. A Cotraining-Based Semisupervised Approach for Remaining-Useful-Life Prediction of Bearings. *Sensors* 2022, 22, 7766.
- [103] Zhao, C.; Huang, X.; Li, Y.; Yousaf Iqbal, M. A Double-Channel Hybrid Deep Neural Network Based on CNN and BiLSTM for Remaining Useful Life Prediction. *Sensors* 2020, 20, 7109.